Journal of Nuclear Medicine, published on June 4, 2021 as doi:10.2967/jnumed.121.262098

An improved ^{211}At-labeled agent for PSMA-targeted alpha therapy

Ronnie C. Mease[1], Choong Mo Kang[2], Vivek Kumar[1], Sangeeta Ray Banerjee[1], Il Minn[1], Mary Brummet[1], Kathleen L. Gabrielson[3], Yutian Feng[2], Andrew Park[1], Ana P. Kiess[4], George Sgouros[1,4], Ganesan Vaidyanathan[2], Michael R. Zalutsky[2], Martin G. Pomper[1,4*]

Institutions: [1]The Russell H. Morgan Department of Radiology and Radiological Science, Johns Hopkins University School of Medicine, Baltimore MD, USA; [2]Department of Radiology, Duke University Medical Center, Durham, NC, USA; [3]Department of Molecular and Comparative Pathobiology Johns Hopkins University School of Medicine, Baltimore MD, USA; [4]Department of Radiation Oncology and Molecular Radiation Sciences, Johns Hopkins University School of Medicine, Baltimore MD, USA.

***Correspondence to:**

Martin G. Pomper, e-mail: mpomper@jhmi.edu, Tel: 410-955-2789

Running Title: ^{211}At-labeled therapy for prostate cancer

Word Count: 6,527

ABSTRACT

α-Particle emitters targeting the prostate-specific membrane antigen (PSMA) proved effective in treating patients with prostate cancer who were unresponsive to the corresponding β-particle therapy. Astatine-211 is an α-emitter that may engender less toxicity than other α-emitting agents. We synthesized a new ^{211}At-labeled radiotracer targeting PSMA that resulted from the search for a pharmacokinetically optimized agent.

Methods: A small series of ^{125}I-labeled compounds were synthesized from their tin precursors to evaluate the effect of location of radiohalogen within the molecule and the presence of lutetium in the chelate on biodistribution. On that basis, ^{211}At-3-Lu was selected and evaluated in cell uptake and internalization studies, biodistribution and PSMA+ PC3 PIP tumor growth control in experimental flank and metastatic (PC3-ML-Luc) models. A long-term (13-month) toxicity study was performed for ^{211}At-3-Lu, including tissue chemistries and histopathology.

Results: The radiochemical yield of ^{211}At-3-Lu was 17.8 ± 8.2%. Lead compound ^{211}At-3-Lu demonstrated total uptake within PSMA+ PC3 PIP cells of 13.4 ± 0.5% of the input dose after 4 h of incubation with little uptake in control cells. In SCID mice, ^{211}At-3-Lu provided 30.6 ± 4.8 percentage of injected dose per gram (%ID/g) of uptake in PSMA+ PC3 PIP tumor at 1 h post-injection that decreased to 9.46 ± 0.96 %ID/g by 24 h. Tumor-to-salivary gland and tumor-to-kidney ratios were 129 ± 99 at 4 h and 130 ± 113 at 24 h, respectively. De-astatination was not significant (stomach 0.34 ± 0.20%ID/g at 4 h). Dose-

dependent survival was demonstrated at higher doses (>1.48 MBq) in both flank and metastatic models. There was little off-target toxicity as demonstrated by hematopoietic stability, unchanged tissue chemistries, weight gain rather than loss throughout treatment, and favorable histopathology.

Conclusion: Compound ^{211}At-3-Lu or close analogs may provide limited and acceptable toxicity while retaining efficacy in management of prostate cancer.

Key words: Prostate cancer, α-emitter, radiopharmaceutical therapy, astatine-211, PSMA, murine models

Radiopharmaceutical therapy targeting prostate-specific membrane antigen (PSMA) using low-molecular-weight agents is becoming a viable treatment for metastatic prostate cancer (*1-3*). Such treatments have utilized β-particle emitters including ^{131}I and ^{177}Lu or α-particle emitters such as ^{213}Bi, ^{212}Pb, ^{227}Th, and ^{225}Ac (*4-10*). To date, most clinical trials have utilized ^{177}Lu. In one such trial, PSA levels decreased by over 50% in 57% of patients (*11*). PSMA-targeted α-particle emitters may be even more promising, as evidenced by treatment with an ^{225}Ac-labeled agent producing significant tumor response in patients that were unresponsive to prior β-emitter therapy (*12,13*). However, the side effect of xerostomia from uptake of the agents in the salivary glands, and the potential of long-term renal toxicity remain possible limitations.

A potential issue with α-emitters like ^{225}Ac is that multiple α-emitting daughters are generated from α-emitting parents, and in each case the energy imparted by the nuclear recoil effect is orders of magnitude greater than chemical bonds. That make the release of the radioactive daughters from the targeting vector extremely likely, which can then lead to unintended irradiation of non-target tissues (*14,15*). Our approach has been to utilize the radiohalogen ^{211}At, which emits a single α-particle per decay. That strategy potentially permits greater control on the targeting of the therapeutic radiation, thereby reducing the chance of off-target effects. It should be noted that 58% of the α-particles emitted during ^{211}At decay do involve a chemical transformation of astatine to polonium before α-emission. In that case, the parent decays by electron capture, not α-emission, so the α-emitting 0.52 sec half-life ^{211}Po daughter is not nuclear-recoil afflicted. Even with worst-possible-case assumptions – that ^{211}Po escapes immediately from the cell surface

and can freely diffuse – nearly 100% of ^{211}Po atoms should decay within two cell diameters from the original cell surface (*16*). The second ^{211}At decay branch (42%) is by direct α-particle emission to ^{207}Bi, which has a 32.9 y half-life. That long-lived radioactive daughter is not of concern because about 100,000 decays of ^{211}At are needed to produce a single atom of ^{207}Bi. Accordingly, a 370 MBq (10 mCi) hypothetical patient dose of a ^{211}At-labeled PSMA agent would yield ~3.7 kBq (~0.1 μCi) ^{207}Bi, a level that is only 0.1% of the Annual Limit of Intake (ALI) recommended for ^{207}Bi by the Nuclear Regulatory Commission 3.7 MBq (100 μCi) (*17*). Despite those issues, we believe ^{211}At remains the best option for α-therapy.

Our previous studies utilized the following compounds shown in Fig. 1, DCABzL, HS-549, GV-620, GV-904, and YC-550. The initial compound studied, ^{211}At-DCABzL, showed high and prolonged uptake in PSMA+ tumor xenografts and renal cortex, with moderate uptake in the thyroid and stomach, likely from dehalogenation (*18*). In spite of that suboptimal biodistribution, we were able to demonstrate a treatment-related increase in survival in both flank tumor xenograft and micrometastatic models with a single dose of 0.74 MBq (20 μCi) and 0.11–0.37 MBq (3-10 μCi), respectively (*18*). From long-term toxicity studies, we determined that the dose-limiting toxicity was late radiation nephropathy (*18*). Using ^{211}At-labeled analogs YC-550, HS-549, GV-904, and GV-620 (Fig. 1), we observed faster renal clearance in mice compared to ^{211}At-DCABzL. However, in vivo dehalogenation and/or off-target organ uptake remained an issue (*19*).

Here we describe a new ^{211}At-labeled PSMA-targeted compound with high stability in vivo, and rapid clearance from off-target tissues in mice including kidneys, salivary and lacrimal glands. We also demonstrate a dose-dependent therapeutic effect in flank xenograft and metastatic tumor models of prostate cancer.

MATERIALS AND METHODS

Reagents, Cell lines and Animal Models

Chemistry. The syntheses of compounds 4 (Fig. 1), and their tin precursor, 15, as well as for unlabeled 3, 3-Lu and their tin precursor 9, are outlined in Figs. 2 and 3, and are described in detail in the Supplemental Materials (Supplemental references *1-4*). The PSMA binding affinity of those compounds was determined using a fluorescence-based assay we have previously reported (*18*).

Radiochemistry. Sodium [^{125}I]iodide in 10 μM NaOH (pH 8-11) was purchased from Perkin Elmer (Waltham, MA). Astatine-211 was produced on the Duke University CS-30 cyclotron via the ^{209}Bi(α,2n)^{211}At reaction on natural bismuth targets (*20,21*)

We investigated 2 methods (A and B) for the preparation of ^{125}I-3-Lu and ^{211}At-3-Lu (Fig 2). Method A included the purification of ^{125}I/^{211}At-3 prior to complexation with ^{175}Lu(III), whereas in Method B Lu complexation was performed in situ without purification of the intermediate. In both methods the final compound was purified by high-performance liquid chromatography (HPLC). Radiosynthesis of ^{211}At-3-Lu by Method B began with a solution

of ^{211}At in 0.02% NCS in methanol [600 µL; 638 MBq (17.3 mCi)] that was added to 310 µg (204 nmol) of 9 in a borosilicate screw cap vial followed by 12 µL of glacial acetic acid. The vial was capped, shaken and allowed to stand at room temperature for 10 min. The reaction mixture was concentrated to dryness using a stream of nitrogen at 60°C. A 95:5 mixture of trifluoroacetic acid:water (200 µL) was added and the vial was heated at 60°C for 30 min. Volatiles were evaporated using a stream of nitrogen at 60°C. Sodium acetate buffer (0.1 M), pH 4.5 (500 µL) and a solution of $Lu(NO_3)_3$ in 0.1 M HCl (65 µL; 325 nmol) were added to the residue and the solution was mixed with a micropipette. That solution was heated at 60°C for 20 min, 100 µL 5 mM EDTA was added, and the reaction mixture was diluted with 600 µL water. The final product was purified by HPLC. For this, a Phenomenex Luna C18 column (250 × 4.6mm, 10 micron) was eluted at a flow rate of 1 mL/min with a gradient consisting of 0.1% TFA in both water (solvent A) and acetonitrile (solvent B). The proportion of B was linearly increased from 15% to 40% over 30 min. Under those conditions, ^{211}At-3-Lu 54 MBq (1.47 mCi) eluted at 22.5 min. Pooled HPLC fractions containing ^{211}At-3-Lu were diluted to 20 mL with water and were loaded onto a Waters Oasis HLB light Sep-Pak. The cartridge was washed with 5 mL water, dried under a stream of nitrogen, and the product was eluted with 0.5 mL ethanol. The eluate was concentrated using a stream of nitrogen and the activity was reconstituted in saline. Detailed radiosyntheses of ^{211}At-3-Lu by Method A, and syntheses of ^{125}I-3, ^{125}I-3-Lu, ^{125}I-4, and ^{125}I-4-Lu are presented in the Supplemental Materials. Radiolabeling yields for ^{125}I/^{211}At-3 and ^{125}I/^{211}At-3-Lu are summarized in Tables 1 and 2.

Cell Lines and Culture Conditions. PSMA-expressing (PSMA+) PC3 PIP and PSMA-negative (PSMA-) PC3 flu cells were maintained as previously described (*22-24*). For the experimental metastatic model, parental PC3-ML-Luc cells were obtained from Dr. Mauricio Reginato (Drexel University). Characterization of those cells is described in Supplemental Fig. 1. Cell lines were maintained mycoplasma-free through bi-weekly testing with the MycoAlert™ mycoplasma detection kit (Lonza, Morristown, NJ).

Animals. Animal studies conformed to protocols approved by the Johns Hopkins Animal Care and Use Committee. Johns Hopkins University has an approved Public Health Service (PHS) Policy and the approved protocols follow the Animal Welfare Act regulations and PHS Policy. NSG (NOD/SCID/IL2Rγnull) mice were obtained from the Animal Resources Core of the Johns Hopkins Sydney Kimmel Comprehensive Cancer Center.

In Vitro Studies

Cell Uptake and Internalization. PSMA+ PC3 PIP cells were plated at 5×10^5 cells/well and incubated overnight. Cells were then incubated with ^{211}At-3 in medium (~3.7 kBq/100 µL) at 37°C for 0.5, 1.0, 2.0 and 4.0 h. Cell culture supernatant was removed and the cells were processed as before (*18*). Cell-associated radioactivity was calculated as percentage of input dose. The internalized fraction of radioactivity was determined by solubilizing cells with 1% SDS cell lysis buffer after removing the unbound fractions and cell surface-bound fractions (by washing with glycine-HCl buffer). To determine binding

specificity, PSMA+ PC3 PIP cells were co-incubated with ^{211}At-3 and the known PSMA inhibitor (*R*, *S*)-2-(phosphonomethyl)pentanedioic acid (2-PMPA; 100 μM) (*25*).

In Vivo Studies

Biodistribution. Six- to 8-week-old male NSG mice were implanted subcutaneously (SC) with PSMA+ PC3 PIP (1.5×10^6) and PSMA- PC3 flu cells (1×10^6) in 100 μL of HBSS (Corning Cellgro, Manassas, VA) at the forward right and left flanks, respectively. Mice were used in ex vivo biodistribution assays when the xenografts reached 5 to 7 mm in diameter. Biodistributions were performed in the above mice bearing both PSMA+ PC3 PIP and PSMA- PC3 flu flank xenografts after an intravenous (IV) bolus of 37 kBq (1 μCi) of either ^{125}I-4, ^{125}I-4-Lu, ^{125}I-3, ^{125}I-3-Lu, or ^{211}At-3-Lu. Tissues harvested at 1, 4, and 24 h post-injection (n=5 per time point) included blood, heart, lung, liver, spleen, pancreas, stomach, small intestine, large intestine, fat, muscle, salivary gland, lacrimal gland, kidney, bladder, PSMA+ PC3 PIP tumor, and PSMA- PC3 flu tumor. Each tissue was weighed, and the associated radioactivity was measured with an automated gamma counter (2480 WIZARD Automatic Gamma Counter, Perkin Elmer, Waltham, MA). The percentage of the injected dose (%ID) was calculated using a known dilution of the %ID. All measurements were corrected for decay. Data are expressed as %ID/g of tissue or per organ (%ID) for organs that were too small for accurate dissection. All data are expressed as mean ± standard deviation (SD).

Antitumor Efficacy in the Subcutaneous Xenograft Model. PSMA+ PC3 PIP and PSMA- PC3 flu cells were implanted SC in male NSG mice as described above. When tumor diameter reached 5 to 7 mm, a single IV injection of ^{211}At-3-Lu was performed with saline, 0.24 MBq (6.6 µCi), 0.74 MBq (20 µCi), 1.48 MBq (40 µCi), or 3.7 MBq (100 µCi) (n=5 per group). Tumor progression was monitored by measuring SC tumor volume [(width^2 x length)/2 mm^3] using a caliper. A tumor volume increase of more than 4-fold was scored as death of the animal, at which point they were euthanized.

Antitumor Efficacy in the Metastatic Model. Four- to 6-week-old NSG mice were injected IV with 1 × 10^6 PC3-ML-Luc cells suspended in 200 µL of HBSS to form micrometastatic deposits. One week post-injection of cells, mice were injected IV with 0, 0.185 MBq (5 µCi), 0.37 MBq (10 µCi), 0.74 MBq (20 µCi), 1.48 MBq (40 µCi), or 3.7 MBq (100 µCi) of ^{211}At-3-Lu (n=5 per group). Metastatic tumor progression was monitored by in vivo bioluminescence imaging (BLI) and survival of injected animals. Weekly BLI was performed using the IVIS Spectrum in vivo Imager (Perkin-Elmer, Waltham, MA). Mice were sacrificed and scored as death if they lost >20% body weight or had signs of discomfort, such as hunched posture, anorexia or dehydration. For both animal models the probability of survival was characterized by Kaplan-Meier curves using GraphPad Prism software (GraphPad Software, San Diego, CA).

Long-term Toxicity. Healthy 11-week-old male CD1 mice (Charles River, Wilmington, MA), weighing 35-40 g received IV injections of 0, 0.24 MBq (6.6 µCi), 0.74 MBq (20 µCi),

or 1.48 MBq (40 μCi) of ^{211}At-3-Lu (n=5 per group). Mice were monitored for 13 months with daily health inspection and weight measurement twice per week. Monthly urinalysis was performed for specific gravity and urine protein content using Chemstrip Test Strips (Roche Diagnostics, Indianapolis IN). After thirteen months, mice were euthanized in a CO_2 chamber, and blood, kidney, salivary and lacrimal glands were collected. Complete blood counts, including white blood cells (WBC), red blood cells (RBC), hemoglobin (HGB), hematocrit (HCT), mean corpuscular volume (MCV), mean corpuscular hemoglobin (MCH), mean corpuscular hemoglobin concentration (MCHC), and platelets (PLT) were measured using the scil Vet ABC™ Hematology Analyzer (scil animal care company, Gurnee, IL). Blood chemistries for blood urea nitrogen (BUN), glucose (GLU), alkaline phosphatase (ALP), total protein (T-Pro), alanine aminotransferase (ALT) and creatinine (Cre) were performed using Spotchem EZ chemistry analyzer (Arkray USA, Edina, MN). Histopathologic evaluation was performed by a certified veterinary pathologist (K.L.G.) for kidney, salivary and lacrimal glands with hematoxylin and eosin (H&E)-stained slides of each tissue.

Statistics

Survival analyses for the metastatic and subcutaneous models were performed using GraphPad Prism 9 software (GraphPad Software, San Diego, CA). *P*-values were calculated by the logrank (Mantel-Cox) test and were considered significant if <0.05.

RESULTS

Chemistry

Because of the promising results obtained with ^{177}Lu-1 and ^{177}Lu-2, our strategy was to replace the non-radioactive bromine or iodine atom with ^{125}I and evaluate their biodistribution in tumor-bearing animals with or without chelated non-radioactive lutetium [^{125}I-3 and ^{125}I-3-Lu (K_i = 0.09 – 34 nM, (*26*)], Fig. 2. For comparison, we also synthesized and evaluated ^{125}I-4 and ^{125}I-4-Lu (Fig. 3), where the radioiodine was incorporated into the linking group, and each contained a 4-bromobenzyl moiety as in 1. The ^{211}At-labeled analog of the most promising iodinated compound was synthesized and evaluated. The binding affinity of unlabeled 3 and 4 were [IC_{50} = 1.51 nM (95% CI: 0.62–3.64 nM); K_i = 0.30 nM (95% CI: 0.13–0.73 nM] and [IC_{50} = 7.82 nM (95% CI: 6.16–9.94 nM); K_i = 0.30 nM (95% CI: 1.23–1.99 nM], respectively.

Radiochemistry

Syntheses of ^{125}I-4 and ^{125}I-4-Lu were each performed once. The yield of ^{125}I-4 from ^{125}I-iodide was 14% and that for the conversion of ^{125}I-4 to ^{125}I-4-Lu was 82%. Radiolabeling conditions and yields for ^{125}I/^{211}At-3 and ^{125}I/^{211}At-3-Lu are given in Tables 1 and 2, respectively. In general, fresh batches of ^{211}At provided higher overall yields of either compound. Purification of the non-metallated intermediate (^{125}I/^{211}At-3) did not enhance yield and actually provided lower overall yields of the final product (^{125}I/^{211}At-3-Lu).

Cell Uptake and Internalization

In vitro studies of ^{211}At-3-Lu demonstrated total uptake within PSMA+ PC3 PIP cells of 13.4 ± 0.5% of the input dose after 4 h of incubation, and an increasing internalized fraction over time, namely, 15.8 ± 0.7%, 19.0 ± 0.7%, 24.5 ± 1.0% and 27.7 ± 2.2% at 0.5, 1.0, 2.0 and 4.0 h, respectively. Co-incubation with 2-PMPA showed an average of 0.6% uptake at all time-points, confirming PSMA-specific binding (Supplemental Fig. 2; Supplemental reference *5*).

Biodistribution

Detailed biodistribution data, represented as %ID/g for all radiolabeled compounds, are given in Supplemental Tables 1-6. There was little de-astatination of ^{211}At-3-Lu in vivo as evidenced by low uptake of radioactivity in stomach (0.39 ± 0.12 %ID/g), salivary glands (0.47 ± 0.19 %ID/g) and spleen (2.51 ± 0.94 %ID/g) at 1 h post-administration, which decreased further by 4 h for stomach and salivary glands (<0.05 %ID/g in spleen) (Supplemental Table 3). Uptake in PSMA+ PC3 PIP tumor and selected non-target organs are shown in Fig. 4. All compounds had high tumor uptake at 1 h (30-60 %ID/g). While tumor activity remained at that high level out to 24 h for ^{125}I-4, ^{125}I-4-Lu and ^{125}I-3, 50% and 67% of ^{125}I-3-Lu and ^{211}At-3-Lu activity, respectively, cleared from the tumor by 24 h. Importantly, ^{211}At-3-Lu was nearly undetectable in normal organs at 24 h. Renal uptake of ^{211}At-3-Lu at 1 h (89.5 ± 42.7 %ID/g) was 30-50% lower than that seen for other compounds. By 4 h, renal activity levels for ^{125}I-3-Lu and ^{211}At-3-Lu decreased to 18.2 ± 3.9 and 2.1 ± 0.6 %ID/g, respectively, while activity in kidneys for the other compounds remained high (162-199 %ID/g). By 24 h, activity in the kidneys from ^{125}I-3-Lu and ^{211}At-

3-Lu decreased to 3.30 ± 1.15 %ID/g and 0.02 ± 0.20 %ID/g, respectively. On the other hand, renal activity was 141 ± 18, 50.4 ± 25.9, and 30.6 ± 14.0 %ID/g for ^{125}I-4, ^{125}I-4-Lu, and ^{125}I-3, respectively. Despite the lower %ID/g values of ^{211}At-3-Lu in tumor, its considerably faster renal clearance resulted in tumor-to-kidney ratios of 8 and 130 at 4 and 24 h, respectively (Fig. 5). Those values are roughly 5- and 16-fold higher than achieved with ^{125}I-3-Lu, and 20- to 200-fold higher compared with the other compounds. The uptake in the spleen at 1 h was much lower for ^{125}I-3-Lu and ^{211}At-3-Lu (7.41 ± 2.57 and 2.51 ± 0.94 %ID/g, respectively) than for the other compounds (40-70 %ID/g). Radioactivity from spleen cleared rapidly for all agents, resulting in tumor/spleen ratios at 4 h of 1.3, 4.4, 6.8, 43, and 97 for ^{125}I-4, ^{125}I-4-Lu, ^{125}I-3, ^{125}I-3-Lu, and ^{211}At-3-Lu, respectively. The uptake of ^{125}I-3-Lu and ^{211}At-3-Lu in the salivary and lacrimal glands was lower than observed for all other compounds at all time-points resulting in tumor-to-salivary gland ratios of 58 and 75 and tumor-to-lacrimal gland ratios of 13 and 44 at 1 h post-injection, respectively (Supplemental Tables 5 and 6, respectively). At 4 h, those values were 365 and 129 for salivary and 92 and 164 for lacrimal glands.

Alpha Therapy with ^{211}At-3-Lu

We first evaluated the efficacy of ^{211}At-3-Lu by scoring growth inhibition of SC xenograft tumors of both PSMA+ PC3 PIP and PSMA- PC3 flu cells implanted in the same animal. Single IV injection of four different doses [0, 0.24 (6.5), 0.74 (20), 1.48 (40), or 3.7 (100) MBq (μCi)] did not affect tumor growth of PSMA- PC3 flu tumors as the median survival of the tumor-bearing mice was 9, 14, 11, 11, and 13 days, respectively. On the other hand, median survival compared to untreated controls for animals harboring PSMA+ PC3

PIP tumors at doses of 0, 0.24 (6.5), 0.74 (20), 1.48 (40), or 3.7 (100) MBq (μCi) were 11 (NS), 27 (*P*=0.0015), 39 (*P*=0.0005), 29 (*P*=0.0005), and not-reached (*P*=0.0005), respectively, indicating that ^{211}At-3-Lu was capable of PSMA-specific tumor growth control and enhancing survival (Fig. 6A). We also tested the efficacy of single dose of IV-administered ^{211}At-3-Lu for treating metastatic deposits of PSMA-expressing tumors. Higher doses (1.48 and 3.7 MBq) provided survival benefits compared with the untreated group (Fig. 6B). Median survival for animals treated with 0, 0.186 (5), 0.373 (10), 0.74 (20), 1.48 (40), or 3.7 (100) MBq (μCi) were 48, 49 (NS), 48 (*P*=0.5769, NS), 52 (*P*=0.0699, NS), 57, (*P*=0.0286) and 58.5 days (*P*=0.2718, due to an early mouse death), respectively.

Long Term Radiotoxicity

Eleven-week-old male CD1 mice were injected with 0.24 MBq (6.6 μCi), 0.74 MBq (20 μCi), or 1.48 MBq (40 μCi) of ^{211}At-3-Lu as a single IV injection. We also included an untreated group for the entire duration of the study as an age-matched control. All groups of mice consistently gained weight for the 13 month-period of monitoring. (Supplemental Fig. 3). Blood chemistry data for all treated groups had similar values for creatinine, BUN, glucose, ALP, ALT, and total protein compared with those for age-matched untreated controls (Supplemental Fig. 4). A complete blood count also indicated that treated groups remained within normal limits (Supplemental Fig. 4). Monthly evaluation of urine protein level (Supplemental Table 7) and specific gravity (Supplemental Table 8) showed no sign of renal impairment compared with untreated controls for the duration of the study. Histopathologic examination of kidney, salivary and lacrimal glands revealed no

treatment-specific pathologic abnormalities at all doses studied (Fig. 7). We observed mild inflammation, a few dilated tubules with protein deposits, and mild multifocal fibrosis in kidneys from all groups (including controls), which were age-related phenomena. Mild age-related inflammation was also observed in salivary and lacrimal glands from all groups.

DISCUSSION

Banerjee et al. reported a series of 4-halobenzyl derivatives of Lys-Glu-urea inhibitors of PSMA containing a linking group that connects the PSMA-targeting urea pharmacophore with a metal chelator (*26*). Two of the most promising compounds were 1 and 2 (Fig. 1). When ^{177}Lu-1 and ^{177}Lu-2 were administered IV to tumor-bearing mice, they exhibited high uptake in PSMA+ PC3 PIP tumor xenografts (*26*), low uptake in the salivary glands, rapid renal clearance, and dose-dependent tumor growth delay. We previously demonstrated in a head-to-head, pre-clinical study that our scaffold bearing the β-particle emitter ^{177}Lu was inferior to that delivering ^{225}Ac, an α-emitter, providing rationale for our focus on PSMA-targeted compounds bearing an α-emitting warhead (*27*).

Reports of PSMA-targeted therapy with the α-emitter ^{225}Ac-PSMA-617 have been encouraging, even in late-stage disease. Some trials report PSA declines of ≥ 90% in roughly half of patients (*28*), and overall survival of > 15 months (*29*). Such results may exceed those of new chemo- or hormonal therapies. However, those results have come at the costs of decreased quality of life, including non-transient, treatment-halting

xerostomia and substantial hematological toxicity according to one retrospective trial (*30*). A greater mitigation of off-target effects, which has proved challenging to date, is needed for PSMA-targeted radiopharmaceutical therapy to develop a niche in management of prostate cancer. Two ways to do so are optimization of pharmacokinetics and choosing the correct α-particle emitter. We have attempted both by focusing on the Type II Lys-Glu-urea scaffold we have previously reported (*26*), a close structural analog of which is currently under investigation in a phase 1-2 clinical trial (NCT0349083800), and on using ^{211}At, which produces only one α-particle per decay and has a tractable physical half-life of 7.2 h (*31-34*).

For convenience of handling, we initially studied the ^{125}I-labeled surrogates of the intended ^{211}At compounds to gauge pharmacokinetics and in vivo stability. Compounds of the 4 series (Fig. 3) enabled us to explore the effect of halogen location in the molecule on pharmacokinetics, as well as the influence of a metal within the chelator, which we previously showed enhanced affinity for PSMA (*26*). While ^{125}I-4 and ^{125}I-4-Lu behaved similarly in PSMA+ PC3 PIP tumor, ^{125}I-4-Lu in kidney substantially decreased by 24 h, indicating a positive effect of the presence of Lu in the chelator on renal clearance. Because even higher tumor-to-kidney ratios were observed for ^{125}I-3-Lu compared with ^{125}I-4-Lu, we continued with the former for further in vivo testing. Relative to ^{125}I-3-Lu, ^{211}At-3-Lu demonstrated lower tumor but also lower off-target uptake. There was also moderate uptake within stomach, consistent with some de-astatination (*35*), however levels remained below 0.5% ID/g and tumor-to-stomach ratios were ~100 (Figs. 4 and 5). By contrast, ^{211}At-DCABzL never had tumor-to-stomach ratios that rose above a few

percent out to 18 h (*18*), and a recently published ^{211}At-labeled minibody targeting prostate cancer only exceeded 1 upon treatment with perchlorate at 5 h (1.2) and 9 h (1.4), post-injection (*36*).

The lack of uptake within stomach and salivary glands of ^{211}At-3-Lu could in part be due to the stability of the low-molecular-weight, Lys-Glu-urea-based targeting scaffold (*37*). There was also little radioactivity in blood (Supplemental Table 3) and no significant change in white blood cell counts (Supplemental Fig. 4). Accordingly, neither treatment with perchlorate (*36*) nor blocking agents were required to mitigate off-target effects. In vivo, ^{211}At-3-Lu treatment caused a PSMA- and dose-dependent increase in survival compared with control animals in both the flank and metastatic models (Fig. 6). Comparison of this result with other reported compounds is challenging due to the different model systems employed. If we focus on our own, earlier therapy studies, we found that ^{211}At-3-Lu provided survival effects at much lower doses than ^{211}At-DCABzL (*18*), which had a maximum tolerated dose (MTD) of 37 kBq (1 μCi). However, that study was performed in nude rather than SCID mice, which we used here. We did not reach the MTD for ^{211}At-3-Lu as the highest dose administered in the long-term (13 month) toxicity study with normal mice was only 1.48 MBq (40 μCi). Nonetheless, even at a dose up to 40 times higher than the MTD for ^{211}At-DCABzL in the same mouse strain, our toxicity data showed only mild changes at all doses and in all organs studied (Fig. 7). Perhaps a more relevant comparison is to ^{225}Ac-L1 (*27*), which demonstrated an MTD of 9.3 kBq (0.25 μCi) (fractionated × 4) because the scaffold is the same as that of ^{211}At-3-Lu. Compound ^{212}Pb-L2 (*38*), which has a similar scaffold, demonstrated an MTD of 1.5 MBq

(~40 μCi). For that compound, there were concerns of long-term renal toxicity, which may be due to the ^{212}Bi daughter released and localized to the kidney, which is not a problem with ^{211}At-based agents.

Our goal in this work was to find a suitable α-particle emitting agent to treat PSMA+ prostate and other cancers that had minimal off-target toxicity, namely, an agent that would be more effective than the corresponding β-particle emitter, but not as toxic as those radiolabeled with ^{225}Ac. We have achieved that with ^{211}At-3-Lu, attesting to the potential benefits of this potentially tamer α-emitter. As with ^{212}Pb, ^{211}At emits only one α-particle per decay. As such, these two radionuclides do not produce daughter α-emissions outside of the intended target site, and will not be expected to have the toxicity, for example, in liver, attendant to such emissions, as those seen with ^{225}Ac. However, there are differences between ^{212}Pb and ^{211}At, which make us favor the latter. The therapeutic potential of ^{212}Pb will be diminished if the daughter nuclei do not remain at the target site so that their energy can also be captured (*7*). For example, Ackerman et al. have calculated that migration of daughters with ^{212}Pb could reduce its relative biological effectiveness to that for conventional external beam radiation and β-particle emitters (*39*). Furthermore, ^{211}At can be introduced to targeting ligands using chemistry very similar to that for other halogens to minimize perturbation of the targeting scaffold if a fastidious cellular target is sought – or a chelator can be deliberately introduced to enhance pharmacokinetics, as in this case (*33,34*). Lack of off-target toxicity, including to salivary and lacrimal glands, would obviate the need for cumbersome co-administration of blocking agents. However, although the natural bismuth target material is inexpensive

and widely available, ^{211}At requires a 28-MeV α-particle cyclotron beam for efficient production, which has curtailed its use (*40*). There are concerted efforts under way to increase the supply of ^{211}At worldwide at academic institutions and research institutes with commercial sources emerging in the not-to-distant future (https://ionetix.com/why-alpha-therapy).

A limitation of this study is the use of cells that may not reflect the natural abundance and heterogeneity of PSMA in human cancer. That issue has been discussed in detail elsewhere (*41*). However, PSMA+ PC3 PIP and PSMA- PC3 flu cells have the advantage of being isogenic, except for PSMA expression, enabling us to answer questions about pharmacokinetics with a minimum of variables present. The superior performance of ^{211}At-3-Lu in the flank rather than the metastatic model may reflect, in part, the supraphysiologic and 10-fold higher PSMA expression in the PSMA+ PC3 PIP cells relative to the PSMA+ PC3-ML-Luc cells used to generate the metastatic deposits (*18*), which express PSMA at about the same level of LNCaP cells (*24*).

CONCLUSION

In this small series, ^{211}At-3-Lu proved to have an excellent combination of properties - a pharmacokinetic profile matching the physical half-life of ^{211}At, ability to effect survival in tumor-bearing animals and lack of off-target toxicity as demonstrated by hematopoietic stability, unchanged tissue chemistries, weight gain rather than loss throughout treatment, and favorable histopathology. This compound or close analogs are promising for

translation if and when an α-particle emitter is to be considered in the therapeutic journey of the patient.

DISCLOSURE

Under a license agreement between D&D Pharmatech and Johns Hopkins and Duke Universities, the Universities R.C.M., M.G.P., S.R.B., G.V. and M.R.Z. are entitled to royalty distributions related to the technology described in the study discussed in this publication. M.G.P., S.R.B. and M.R.Z. hold equity in D&D Pharmatech; M.G.P. and S.R.B. are co-founders. They and M.R.Z. are also paid consultants to the company. This arrangement has been reviewed and approved by Johns Hopkins University and Duke University in accordance with their conflict of interest policies.

ACKNOWLEDGMENTS

We thank CA184228, EB024495 and CA134675 and the Commonwealth Foundation for financial support.

KEY POINTS

QUESTION: Can a PSMA-targeted, α-emitting small molecule be designed with few off-target toxic effects while retaining therapeutic efficacy?

PERTINENT FINDINGS: Lead compound ^{211}At-3-Lu was able to control tumor growth and enhance survival in animals treated at doses of 1.48 MBq or greater, and did so without toxicity.

IMPLICATIONS FOR PATIENT CARE: Compounds such as ^{211}At-3-Lu provide further rationale for the use of ^{211}At in targeted α-emitting radiopharmaceuticals. Astatine-211 may be an effective and non-toxic alternative to other α-emitters in use for management of prostate and other PSMA-expressing cancers. Its ease of incorporation to a variety of cancer affinity agents, including small molecules, as well as its convenient physical half-life could provide a safe, practical, and new method to treat a variety of intractable malignancies.

REFERENCES

1. Miyahira AK, Pienta KJ, Babich JW, et al. Meeting report from the Prostate Cancer Foundation PSMA theranostics state of the science meeting. *Prostate.* 2020;80:1273-1296.

2. Jones W, Griffiths K, Barata PC, Paller CJ. PSMA Theranostics: Review of the Current Status of PSMA-Targeted Imaging and Radioligand Therapy. *Cancers (Basel).* 2020;12.

3. O'Dwyer E, Bodei L, Morris MJ. The Role of Theranostics in Prostate Cancer. *Semin Radiat Oncol.* 2021;31:71-82.

4. Zechmann CM, Afshar-Oromieh A, Armor T, et al. Radiation dosimetry and first therapy results with a (124)I/ (131)I-labeled small molecule (MIP-1095) targeting PSMA for prostate cancer therapy. *Eur J Nucl Med Mol Imaging.* 2014;41:1280-1292.

5. Kratochwil C, Giesel FL, Stefanova M, et al. PSMA-Targeted Radionuclide Therapy of Metastatic Castration-Resistant Prostate Cancer with 177Lu-Labeled PSMA-617. *J Nucl Med.* 2016;57:1170-1176.

6. Morgenstern A, Apostolidis C, Kratochwil C, Sathekge M, Krolicki L, Bruchertseifer F. An Overview of Targeted Alpha Therapy with (225)Actinium and (213)Bismuth. *Curr Radiopharm.* 2018;11:200-208.

7. Dos Santos JC, Schafer M, Bauder-Wust U, et al. Development and dosimetry of (203)Pb/(212)Pb-labelled PSMA ligands: bringing "the lead" into PSMA-targeted alpha therapy? *Eur J Nucl Med Mol Imaging.* 2019;46:1081-1091.

8. Hammer S, Hagemann UB, Zitzmann-Kolbe S, et al. Preclinical Efficacy of a PSMA-Targeted Thorium-227 Conjugate (PSMA-TTC), a Targeted Alpha Therapy for Prostate Cancer. *Clin Cancer Res.* 2020;26:1985-1996.

9. Kratochwil C, Bruchertseifer F, Giesel FL, et al. 225Ac-PSMA-617 for PSMA-Targeted alpha-Radiation Therapy of Metastatic Castration-Resistant Prostate Cancer. *J Nucl Med.* 2016;57:1941-1944.

10. Yadav MP, Ballal S, Sahoo RK, Tripathi M, Seth A, Bal C. Efficacy and safety of (225)Ac-PSMA-617 targeted alpha therapy in metastatic castration-resistant Prostate Cancer patients. *Theranostics.* 2020;10:9364-9377.

11. Hofman MS, Violet J, Hicks RJ, et al. [(177)Lu]-PSMA-617 radionuclide treatment in patients with metastatic castration-resistant prostate cancer (LuPSMA trial): a single-centre, single-arm, phase 2 study. *Lancet Oncol.* 2018;19:825-833.

12. Zacherl MJ, Gildehaus FJ, Mittlmeier L, et al. First clinical results for PSMA targeted alpha therapy using (225)Ac-PSMA-I&T in advanced mCRPC patients. *J Nucl Med.* 2020.

13. Ilhan H, Gosewisch A, Boning G, et al. Response to (225)Ac-PSMA-I&T after failure of long-term (177)Lu-PSMA RLT in mCRPC. *Eur J Nucl Med Mol Imaging.* 2021;48:1262-1263.

14. de Kruijff RM, Wolterbeek HT, Denkova AG. A Critical Review of Alpha Radionuclide Therapy-How to Deal with Recoiling Daughters? *Pharmaceuticals (Basel).* 2015;8:321-336.

15. Kozempel J, Mokhodoeva O, Vlk M. Progress in Targeted Alpha-Particle Therapy. What We Learned about Recoils Release from In Vivo Generators. *Molecules.* 2018;23.

16. Palm S, Humm JL, Rundqvist R, Jacobsson L. Microdosimetry of astatine-211 single-cell irradiation: role of daughter polonium-211 diffusion. *Med Phys.* 2004;31:218-225.

17. US Nuclear Regulatory Commission Report NRC, 10CFR. https://www.nrc.gov/reading-rm/doc-collections/cfr/part020/appb/bismuth-207.html.

18. Kiess AP, Minn I, Vaidyanathan G, et al. (2S)-2-(3-(1-Carboxy-5-(4-211At-Astatobenzamido)Pentyl)Ureido)-Pentanedioic Acid for PSMA-Targeted alpha-Particle Radiopharmaceutical Therapy. *J Nucl Med.* 2016;57:1569-1575.

19. Vaidyanathan G, Mease RC, Minn I, et al. Synthesis and preliminary evaluation of (211)At-labeled inhibitors of prostate-specific membrane antigen for targeted alpha particle therapy of prostate cancer. *Nucl Med Biol.* 2021;94-95:67-80.

20. Zalutsky MR, Zhao XG, Alston KL, Bigner D. High-level production of alpha-particle-emitting (211)At and preparation of (211)At-labeled antibodies for clinical use. *J Nucl Med.* 2001;42:1508-1515.

21. Pozzi OR, Zalutsky MR. Radiopharmaceutical chemistry of targeted radiotherapeutics, Part 3: alpha-particle-induced radiolytic effects on the chemical behavior of (211)At. *J Nucl Med.* 2007;48:1190-1196.

22. Nakajima T, Mitsunaga M, Bander NH, Heston WD, Choyke PL, Kobayashi H. Targeted, activatable, in vivo fluorescence imaging of prostate-specific membrane antigen (PSMA) positive tumors using the quenched humanized J591 antibody-indocyanine green (ICG) conjugate. *Bioconjug Chem.* 2011;22:1700-1705.

23. Chang SS, Reuter VE, Heston WD, Bander NH, Grauer LS, Gaudin PB. Five different anti-prostate-specific membrane antigen (PSMA) antibodies confirm PSMA expression in tumor-associated neovasculature. *Cancer Res.* 1999;59:3192-3198.

24. Kiess AP, Minn I, Chen Y, et al. Auger Radiopharmaceutical Therapy Targeting Prostate-Specific Membrane Antigen. *J Nucl Med.* 2015;56:1401-1407.

25. Jackson PF, Cole DC, Slusher BS, et al. Design, synthesis, and biological activity of a potent inhibitor of the neuropeptidase N-acetylated alpha-linked acidic dipeptidase. *J Med Chem.* 1996;39:619-622.

26. Banerjee SR, Kumar V, Lisok A, et al. (177)Lu-labeled low-molecular-weight agents for PSMA-targeted radiopharmaceutical therapy. *Eur J Nucl Med Mol Imaging.* 2019;46:2545-2557.

27. Ray S, Lisok A, Minn IL, et al. Preclinical evaluation of (213)Bi-/(225)Ac-labeled low-molecular-weight compounds for radiopharmaceutical therapy of prostate cancer. *J Nucl Med.* 2020.

28. Sathekge M, Bruchertseifer F, Knoesen O, et al. (225)Ac-PSMA-617 in chemotherapy-naive patients with advanced prostate cancer: a pilot study. *Eur J Nucl Med Mol Imaging.* 2019;46:129-138.

29. Sathekge M, Bruchertseifer F, Vorster M, et al. Predictors of Overall and Disease-Free Survival in Metastatic Castration-Resistant Prostate Cancer Patients Receiving (225)Ac-PSMA-617 Radioligand Therapy. *J Nucl Med.* 2020;61:62-69.

30. Feuerecker B, Tauber R, Knorr K, et al. Activity and Adverse Events of Actinium-225-PSMA-617 in Advanced Metastatic Castration-resistant Prostate Cancer After Failure of Lutetium-177-PSMA. *Eur Urol.* 2021;79:343-350.

31. Lindegren S, Albertsson P, Back T, Jensen H, Palm S, Aneheim E. Realizing Clinical Trials with Astatine-211: The Chemistry Infrastructure. *Cancer Biother Radiopharm.* 2020;35:425-436.

32. Meyer GJ. Astatine. *J Labelled Comp Radiopharm.* 2018;61:154-164.

33. Vaidyanathan G, Zalutsky MR. Astatine Radiopharmaceuticals: Prospects and Problems. *Curr Radiopharm.* 2008;1:177.

34. Guerard F, Gestin JF, Brechbiel MW. Production of [(211)At]-astatinated radiopharmaceuticals and applications in targeted alpha-particle therapy. *Cancer Biother Radiopharm.* 2013;28:1-20.

35. Larsen RH, Slade S, Zalutsky MR. Blocking [211At]astatide accumulation in normal tissues: preliminary evaluation of seven potential compounds. *Nucl Med Biol.* 1998;25:351-357.

36. Back TA, Jennbacken K, Hagberg Thulin M, et al. Targeted alpha therapy with astatine-211-labeled anti-PSCA A11 minibody shows antitumor efficacy in prostate cancer xenografts and bone microtumors. *EJNMMI Res.* 2020;10:10.

37. Pomper MG, Musachio JL, Zhang J, et al. 11C-MCG: synthesis, uptake selectivity, and primate PET of a probe for glutamate carboxypeptidase II (NAALADase). *Mol Imaging.* 2002;1:96-101.

38. Banerjee SR, Minn I, Kumar V, et al. Preclinical Evaluation of (203/212)Pb-Labeled Low-Molecular-Weight Compounds for Targeted Radiopharmaceutical Therapy of Prostate Cancer. *J Nucl Med.* 2020;61:80-88.

39. Ackerman NL, de la Fuente Rosales L, Falzone N, Vallis KA, Bernal MA. Targeted alpha therapy with (212)Pb or (225)Ac: Change in RBE from daughter migration. *Phys Med.* 2018;51:91-98.

40. Zalutsky MR, Pruszynski M. Astatine-211: production and availability. *Curr Radiopharm.* 2011;4:177-185.

41. Current K, Meyer C, Magyar CE, et al. Investigating PSMA-Targeted Radioligand Therapy Efficacy as a Function of Cellular PSMA Levels and Intratumoral PSMA Heterogeneity. *Clin Cancer Res.* 2020;26:2946-2955.

Figure 1

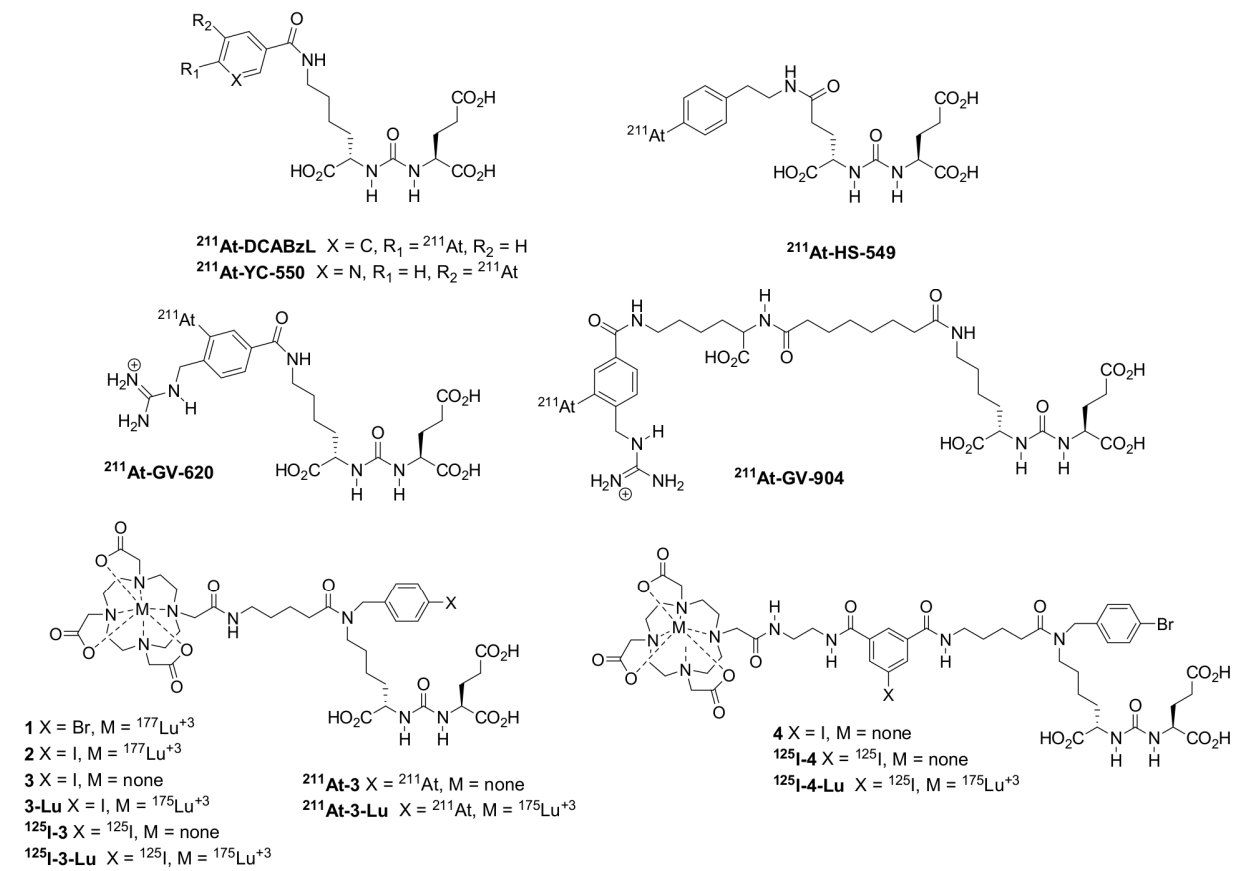

PSMA-targeted agents.

Figure 2

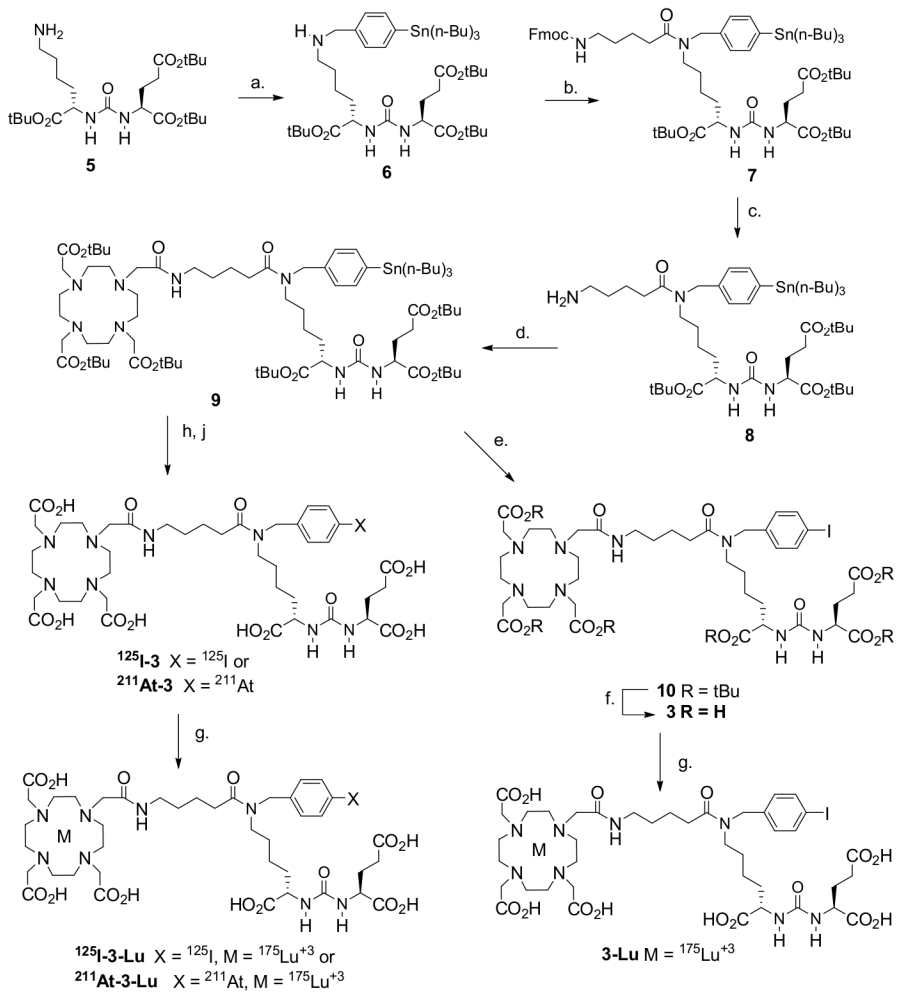

Synthesis of 3, 3-Lu, radiolabeling precursor 9, ^{125}I-3, ^{125}I-3-Lu, and ^{211}At-3-Lu. Reagents and conditions: a. 4-(Tributylstannyl)benzaldehyde, methanol, sodium cyanoborohydride; b. 5-(Fmoc-amino)valeric acid, TSTU, DIPEA, DMF; c. 20% piperidine in DMF; d. DOTA-NHS tri-tert-butylester, DIPEA, DMSO; e. I_2, CH_2Cl_2; f. 1/1 TFA/CH_2Cl_2; g. i. 0.2 M NH_4OAc, DMSO, 5 mM $^{175}Lu(NO_3)_3{\cdot}H_2O$ in 0.1 N HCl, 70^{o}C 20 min, ii. EDTA; h. Na^{125}I or ^{211}At, methanol, glacial acetic acid, room temperature, 20 min; j. trifluoroacetic acid, 60-70^{o}C, 30-45 min.

Figure 3

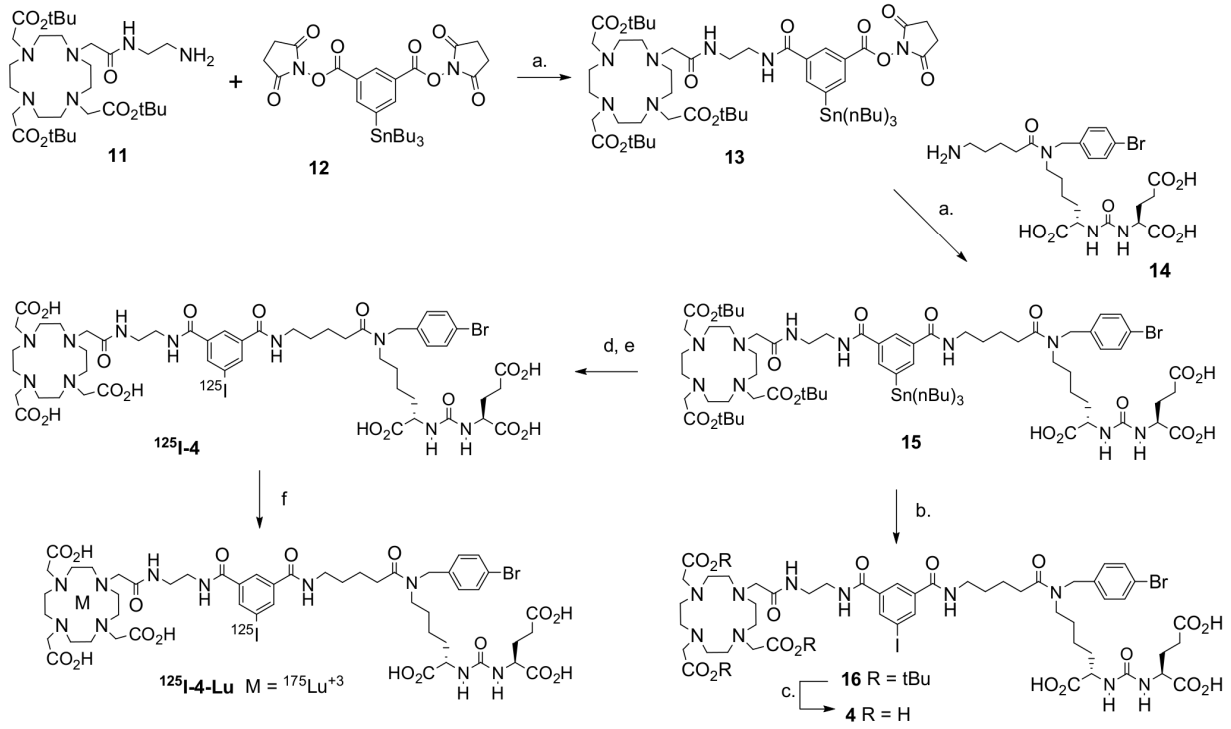

Synthesis of Radiolabeling precursor 15, 4, ^{125}I-4 and ^{125}I-4-Lu. Reagents and conditions: a. triethylamine, DMSO, room temperature, 2 h; b. I_2, CH_2Cl_2, room temperature, 2 h; c. 1/1 trifluoroacetic acid/CH_2Cl_2,room temperature, 2 h; d. Na^{125}I, N-chlorosuccinimide, glacial acetic acid, methanol, room temperature, 20 min; e. concentrated formic acid, 60^{o}C, 1 h; f. i. 0.1 M sodium acetate, pH 4.5, 5 mM $^{175}Lu(NO_3)_3$ in 0.1 M HCl, 60^{o}C, 20 min, ii. 5 mM EDTA.

Figure 4

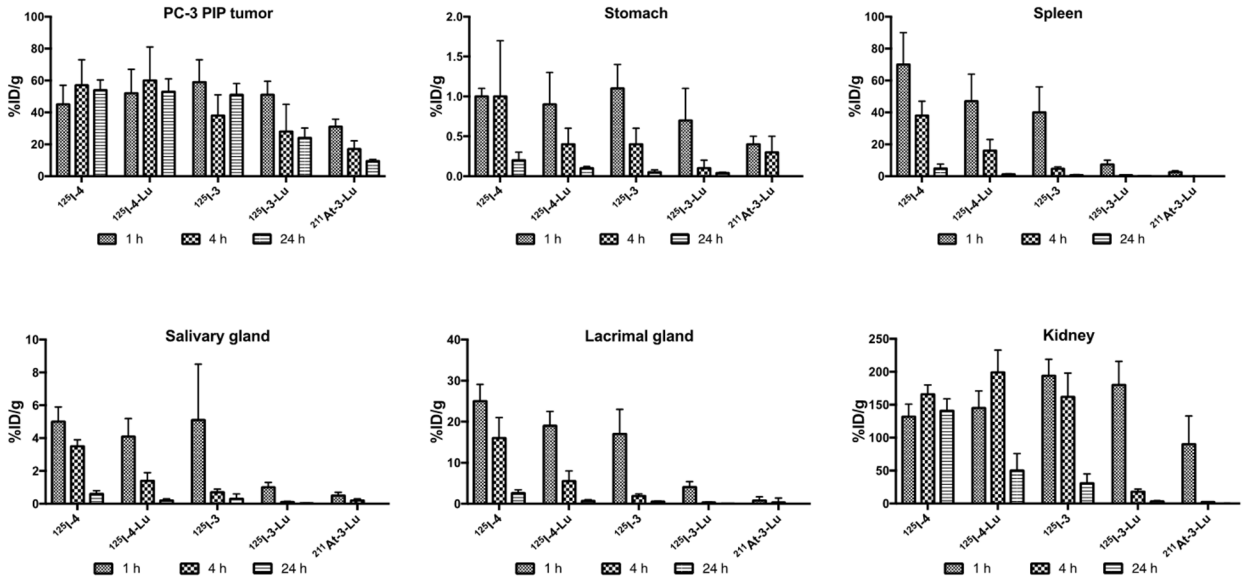

Biodistribution of radiolabeled compounds of Fig. 2 and 3 in selected tissues presented as percentage of injected dose per gram of tissue (%ID/g).

Figure 5

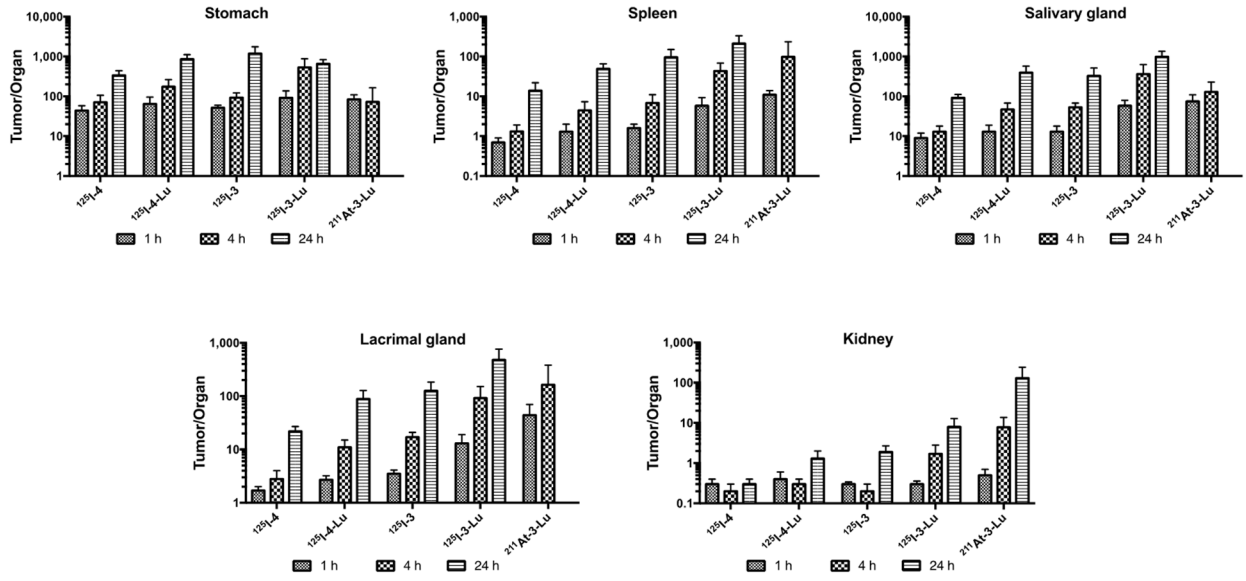

Biodistribution of compounds of Fig. 2 and 3 in selected tissues presented as ratios of tumor to selected organs.

Figure 6

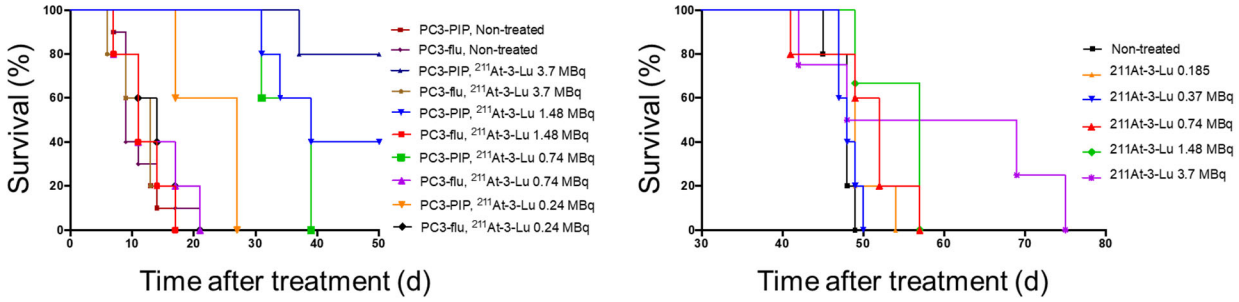

Kaplan-Meier curves showing survival in the flank (A) and PC3-ML-Luc experimental metastatic (B) models at the does provided. PC3-PIP = PSMA+ PC3 PIP and PC3-flu = PSMA- PC3 flu cell derived tumors.

Figure 7

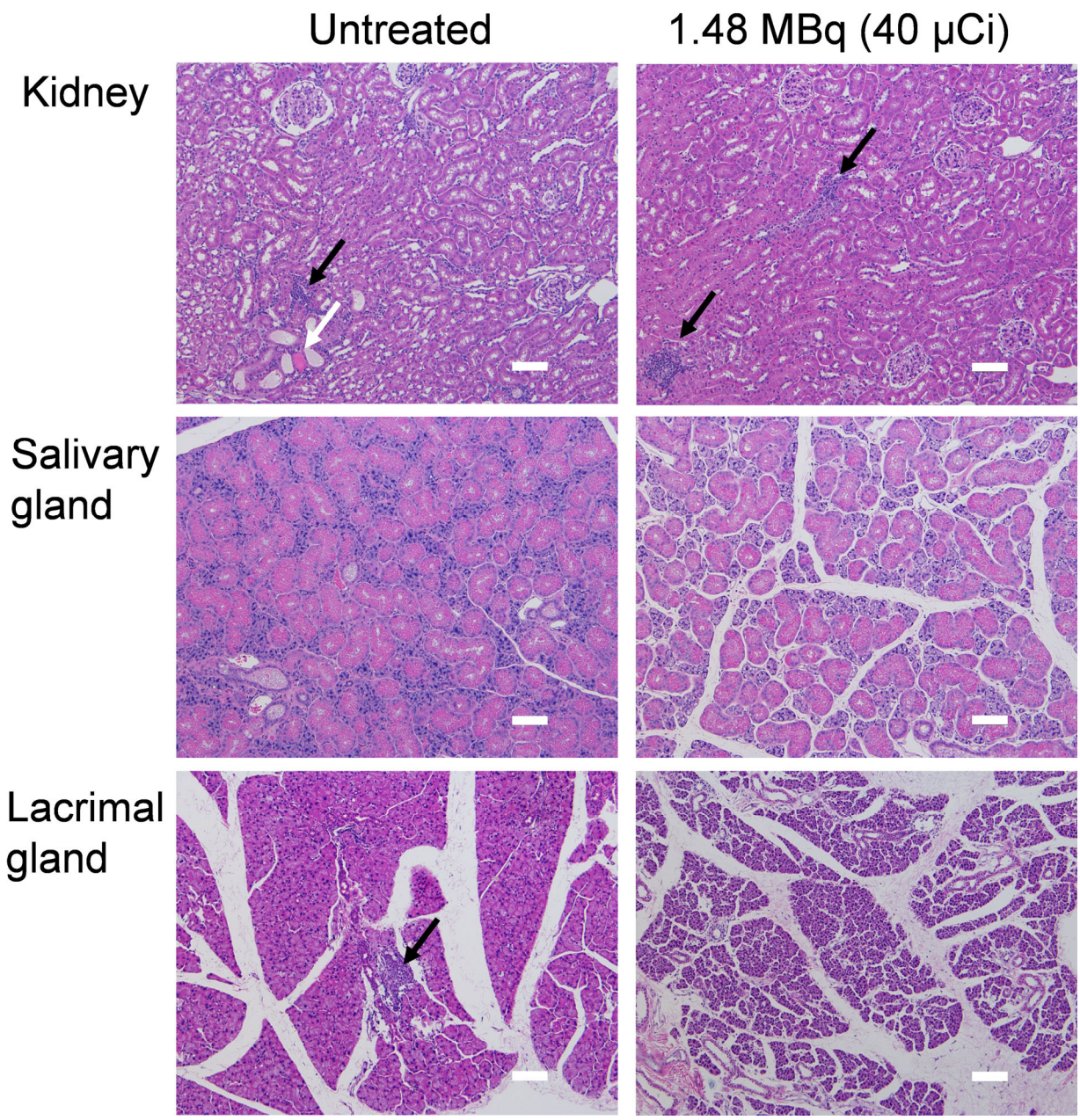

Representative microscopic images of kidney, salivary gland, and lacrimal gland. Size bar = 100 μm. Black arrow: inflammation, white arrow: dilated tubule with protein deposit.

Table 1. Radiolabeling yields for $^{125}I/^{211}At$-3

Radionuclide	Starting Radioactivity	Age of ^{211}At	N	% Yield[a]
^{125}I	0.036-0.266 GBq (0.96-7.2mCi)	NA	3	56.1 ±13.7
^{211}At	0.1628-0.3145 GBq (4.4-8.5 mC)i	Fresh	3	49.6 ±6.8
^{211}At	0.444-0.6623 GBq (12.0-17.9 mCi)	≥9 Hours	2	20.8 ±8.2%

a. After Preparative HPLC Purification

Table 2. Radiolabeling yields for $^{125}I/^{211}At$-3-Lu

Radio-nuclide	Starting Radioactivity	Age of ^{211}At	Method of Preparation	N	Yield[a]
^{125}I	0.170-0.266GBq (4.6-7.2mCi)	NA	A	2	46.5 ±7.7%
^{125}I	0.054-0.518GBq (1.47-14mCi)	NA	B	4	62.8 ±9.0%
^{211}At	0.16 – 0.31GBq (4.4-8.5mCi)	Fresh	A	3	6.3 ±1.8%
^{211}At	0.126- 0.34GBq (3.4-9.2mCi)	Fresh	B	2	17.8 ± 8.2%
^{211}At	0.44 – 0.66GBq (12.0-17.0mCi)	≥ 9 Hours	A	2	8.6 ± 3.6%
^{211}At	0.115 – 0.877GBq (3.1-23.7mCi)	≥ 9 Hours	B	4	13.6 ± 8.4%

a. After Preparative HPLC Purification
Method A: Separate Preparative HPLC purification of $^{125}I/^{211}At$-3 and $^{125}I/^{211}At$-3-Lu
Method B: Preparative HPLC purification of $^{125}I/^{211}At$-3-Lu only.

Graphical Abstract

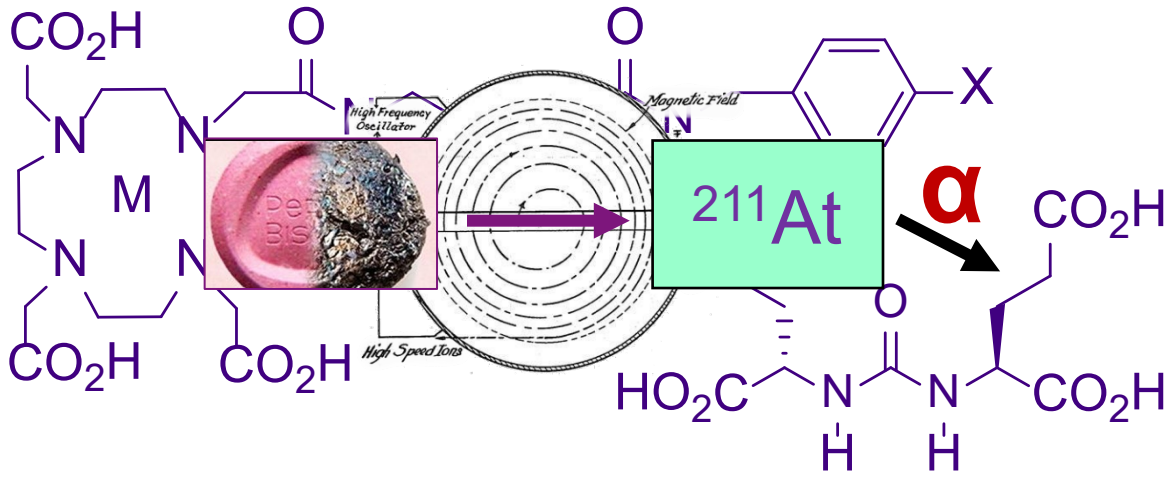

Supplemental References

1. Sessler, J.L., Wang, B. Harriman, A.,, *Photoinduced energy transfer in associated but noncovalently linked Photosynthetic model system.* Journal of the American Chemical Society, 1995. **117**: p. 704-714.

2. Maresca, K.P., et al., *A series of halogenated heterodimeric inhibitors of prostate specific membrane antigen (PSMA) as radiolabeled probes for targeting prostate cancer.* J Med Chem, 2009. **52**(2): p. 347-57.

3. Vaidyanathan, G., et al., *SIB-DOTA: a trifunctional prosthetic group potentially amenable for multi-modal labeling that enhances tumor uptake of internalizing monoclonal antibodies.* Bioorg Med Chem, 2012. **20**(24): p. 6929-39.

4. Banerjee, S.R., et al., *(177)Lu-labeled low-molecular-weight agents for PSMA-targeted radiopharmaceutical therapy.* Eur J Nucl Med Mol Imaging, 2019. **46**(12): p. 2545-2557.

5. Kiess, A.P., et al., *(2S)-2-(3-(1-Carboxy-5-(4-211At-Astatobenzamido)Pentyl)Ureido)-Pentanedioic Acid for PSMA-Targeted alpha-Particle Radiopharmaceutical Therapy.* J Nucl Med, 2016. 57(10): p. 1569-1575.

Chemistry

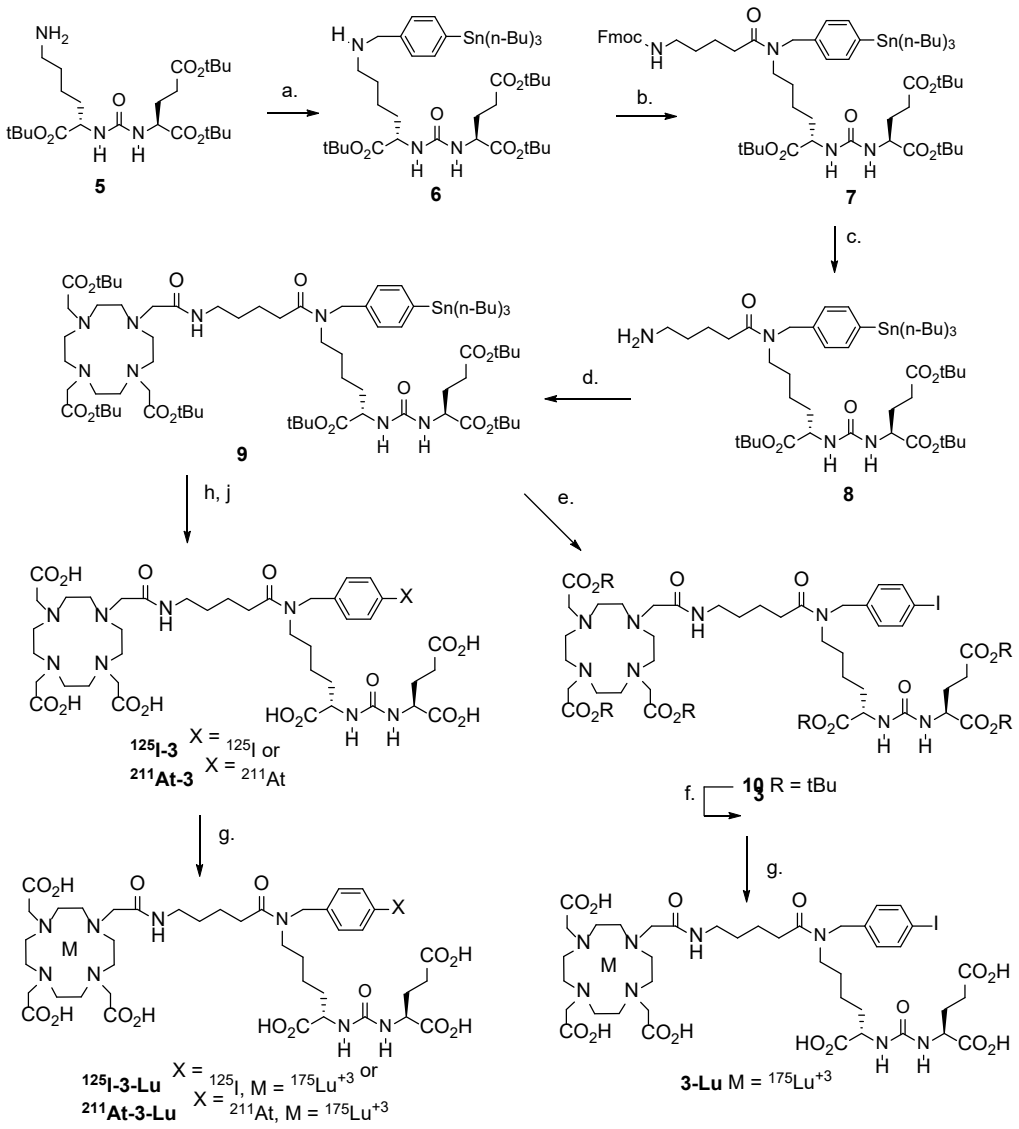

Synthesis of **3**, **3-Lu**, radiolabeling precursor **9**, **^{125}I-3**, **^{125}I-3-Lu**, and **^{211}At-3-Lu**. Reagents and conditions. a. 4-(tributylstannyl)benzaldehyde, methanol, sodium cyanoborohydride; b.5-(Fmoc-amino)valeric acid, TSTU, DIPEA, DMF; c. 20% piperidine in DMF; d. DOTA-NHS tri-t-butylester, DIPEA, DMSO; e. I_2, CH_2Cl_2; f. 1/1 TFA/CH_2Cl_2; g. i. 0.2M NH_4OAc, DMSO, 5mM $^{175}Lu(NO_3)_3.xH_2O$ in 0.1N HCl, 70^{o}C 20 min., ii. EDTA; h. $Na^{125}I$ or ^{211}At, methanol, glacial acetic acid, room temp. 20 min; j. trifluoroacetic acid, 60-70^{o}C, 30-45 min,

Di-tert-butyl (((*S*)-1-(tert-butoxy)-1-oxo-6-((4-(tri-n-butylstannyl)benzyl)amino)hexan-2-yl)carbamoyl)-*L*-glutamate (6)

A solution of 4-(tri-n-butylstannyl)benzaldehyde [1] (0.50 g, 1.26 mmol, in 5 ml MeOH) was added dropwise to a stirred solution of urea **5** [2] (0.61 g, 1.26 mmol) in MeOH (5 ml) at 0-5°C under a nitrogen atmosphere. The reaction mixture was stirred at RT for 1 h and then treated with sodium cyanoborohydride (0.32 g, 5.05 mmol). The mixture was stirred overnight at RT and concentrated under vacuum. Purification by silica gel flash column chromatography using 40-50% EtOAc/Hexanes as the mobile phase provided 0.54 g (49%) of an oily material. ^{1}H NMR ($CDCl_3$)

δ ppm 7.48 (d, *J* = 10.0 Hz, 2H), 7.36 (d, *J* = 5.0 Hz, 2H), 5.92 (m, 1H), 5.73 (m, 1H), 4.26-4.23 (m, 1H), 4.07-4.00 (m, 2H), 2.87-2.84 (m, 2H), 2.29 (t, *J* = 5.0 Hz, 2H), 1.91-1.87 (m, 1H), 1.80-1.78 (m, 1H), 1.72-1.70 (m, 2H), 1.59-1.55 (m, 1H), 1.53-1.49 (m, 5H), 1.45-1.41 (m, 27H), 1.34-1.26 (m, 7H), 1.25-1.22 (m, 3H), 1.05-1.02 (m, 6H), 0.86 (t, *J* = 5.0 Hz, 9H); ^{13}C NMR ($CDCl_3$) δ ppm 173.4, 172.5, 172.4, 172.2, 157.8, 143.9, 137.2, 137.0, 129.2, 82.6, 81.8, 80.6, 53.8, 53.5, 53.1, 51.9, 46.9, 31.7, 31.6, 29.7, 29.0, 28.1, 28.0, 27.3, 26.9, 26.1, 22.9, 13.7, 9.6.ESI-MS *m*/*z*: 868.4 $(M + H)^+$.

Tri-tert-butyl (15*S*, 19*S*)-1-(9H-fluoren-9-yl)-3,9,17-trioxo-10-(4-(tri-n-butylstannyl)benzyl)-2-oxa-4,10,16,18-tetraazahenicosane-15,19,21-tricarboxylate (7)

A mixture of 5-(Fmoc-amino)valeric acid (0.02 g, 0.06 mmol), TSTU (0.02 g, 0.06 mmol) and DIPEA (0.02 g, 0.11 mmol) was stirred in DMF (1 ml) at RT for 1 h. A solution of **6** (0.05 g, 0.06 mmol) in DMF (1 ml) was added dropwise to the above. The reaction mixture was stirred for 4 h, concentrated and purified by silica gel flash column chromatography using 40-50% EtOAc/Hexanes as the mobile phase to provide 0.54 g (47%) of an oily material. ^{1}H NMR ($CDCl_3$) δ ppm 7.76 (d, *J* = 10.0 Hz, 3H), 7.60 (d, *J* = 5.0 Hz, 3H), 7.40 (m, 4H), 7.31 (m, 4H), 4.99 (bs, 1H), 4.40 (m, 3H), 4.21 (m, 1H), 3.23 (q, *J* = 5.0 Hz, 3H), 2.83 (m, 5H), 2.66-2.63 (m, 2H), 2.36-2.29 (m, 1H), 1.89-1.81 (m, 1H), 1.80-1.75 (m, 4H), 1.65-1.62 (m, 4H), 1.55-1.52 (m, 4H), 1.45-1.42 (m, 14H), 1.36-1.23 (m, 20H), 1.11-1.01 (m, 4H), 0.97 (d, *J* = 5.0 Hz, 1H), 0.90-0.86 (m, 11H); ^{13}C NMR ($CDCl_3$) δ ppm 169.2, 168.4, 156.5, 144.0, 141.3, 136.9, 127.7, 127.0, 125.1, 119.9, 66.5, 47.3, 40.3, 34.7, 31.6, 30.9, 29.7, 29.1, 28.1, 28.0, 27.4, 27.3, 25.6, 25.3, 22.7, 21.8, 18.8, 14.2, 13.7, 11.5, 9.6. ESI-MS m/z: 910.4 (M – Fmoc - butyl + H)$^+$, 676.5 (M – Fmoc – Sn(n-Bu)$_3$)$^+$.

Di-*tert*-butyl (((*S*)-6-(5-amino-*N*-(4-(tributylstannyl)benzyl)pentanamido)-1-(*tert*-butoxy)-1-oxohexan-2-yl)carbamoyl)-*L*-glutamate (8)

A solution of 20% piperidine/DMF (2.5 ml) was added to **7** (0.32 g, 0.27 mmol) and stirred at RT for 2.5 h. The reaction mixture was concentrated and purified using a silica gel flash chromatography column eluted with 10% MeOH/CH_2Cl_2/NH_4OH. Lyophilization of chromatography fractions provided 0.190 g (74%) of an oily product. ^{1}H NMR ($CDCl_3$) δ ppm 7.44 (d, *J* = 5.0 Hz, 1H), 7.38 (d, *J* = 5.0 Hz, 1H), 7.14 (d, *J* = 5.0 Hz, 1H), 7.08 (d, *J* = 5.0 Hz, 1H), 6.25 (m, 1H), 6.14-6.11 (m, 1H), 4.61-4.49 (m, 1H), 4.48-4.44 (m, 1H), 4.32-4.27 (m, 2H), 3.54-3.50 (m, 1H), 3.41 (m, 1H), 3.29-3.18 (m, 2H), 3.06-3.03 (m, 2H), 2.68 (m, 1H), 2.49-2.36 (m, 2H), 2.35-2.30 (m, 3H), 2.06-2.04 (m, 1H), 1.87-1.73 (m, 8H), 1.60-1.49 (m, 7H), 1.43-1.42 (m, 27H), 1.35-1.27 (m, 8H), 1.05-1.00 (m, 6H), 0.87 (t, *J* = 10.0 Hz, 9H); ^{13}C NMR ($CDCl_3$) δ ppm 173.9, 173.0, 172.8, 172.7, 157.5, 157.3, 141.3, 140.7, 137.0, 136.7, 136.2, 127.5, 125.8, 81.9, 81.8, 81.4, 80.6, 53.6, 52.9, 50.6, 47.8, 46.6, 45.1, 40.5, 32.7, 31.8, 29.7, 29.2, 29.1, 28.1, 27.4, 27.2, 26.9, 22.5, 21.9, 13.7, 9.6. ESI-MS *m*/*z*: 967.3 $(M + H)^+$.

Tri-*tert*-butyl (14*S*,18*S*)-2,8,16-trioxo-9-(4-(tributylstannyl)benzyl)-1-(4,7,10-tris(2-(*tert*-butoxy)-2-oxoethyl)-1,4,7,10-tetraazacyclododecan-1-yl)-3,9,15,17-tetraazaicosane-14,18,20-tricarboxylate (9)

A mixture of DOTA-NHS-ester (0.028 g, 0.03 mmol), **8** (0.03 g, 0.03 mmol) and DIPEA (0.04 g, 0.31 mmol) in DMSO (1 ml) was stirred at RT for 3 h. The reaction mixture was concentrated and purified by silica gel flash chromatography using 1.5% MeOH/CH_2Cl_2 as the mobile phase to provide 0.024 g (51%) of an oily product. ^{1}H NMR ($CDCl_3$) δ ppm 7.40 (d, *J* = 5.0 Hz, 1H), 7.35

(d, *J* = 10.0 Hz, 1H), 7.11 (d, *J* = 10.0 Hz, 1H), 7.07 (d, *J* = 10.0 Hz, 1H), 6.56-6.52 (m, 1H), 6.15 (bs, 1H), 5.59 (d, *J* = 10.0 Hz, 1H), 5.42 (d, *J* = 5.0 Hz, 1H), 4.50 (d, *J* = 10.0 Hz, 2H), 4.30-4.21 (m, 2H), 3.72-3.64 (m, 1H), 3.35-3.30 (m, 3H), 3.22-3.12 (m, 5H), 2.84 (m, 6H), 2.39 (m, 2H), 2.33-2.25 (m, 6H), 2.04-2.01 (m, 3H), 1.85 (m, 1H), 1.69-1.58 (m, 4H), 1.57-1.47 (m, 10H), 1.44-1.38 (m, 59H), 1.34-1.26 (m, 9H), 1.03-0.98 (m, 6H), 0.85 (t, *J* = 10.0 Hz, 9H); ^{13}C NMR ($CDCl_3$) δ ppm 173.5, 173.1, 172.9, 172.5, 172.4, 172.1, 171.4, 171.3, 169.7, 157.1, 157.0, 141.1, 140.5, 137.5, 136.9, 136.6, 136.5, 127.4, 125.8, 82.2, 81.9, 81.8, 81.7, 81.6, 56.0, 55.7, 53.2, 53.1, 52.9, 50.9, 48.1, 46.9, 45.5, 39.2, 39.1, 32.8, 32.6, 31.8, 31.7, 30.9, 29.1, 28.1, 28.0, 27.9, 27.8, 27.4, 26.6, 25.6, 22.6, 22.5, 22.4, 13.7, 9.6. ESI-MS *m*/*z*: 761.3 $(M/2 + H)^+$.

Tri-*tert*-butyl (14*S*, 18*S*)-9-(4-iodobenzyl)-2,8,16-trioxo-1-(4,7,10-tris(2-(*tert*-butoxy)-2-oxoethyl)-1,4,7,10-tetraazacyclododecan-1-yl)-3,9,15,17-tetraazaicosane-14,18,20-tricarboxylate (10)

Iodine (0.012 g, 0.094 mmol) was added to a solution of **9** (0.05 g, 0.03 mmol) in CH_2Cl_2 (2 ml) and stirred at RT for 2h. The reaction mixture was washed with 10% aqueous $Na_2S_2O_5$ solution, dried, concentrated and purified by silica gel flash chromatography using 1.5% MeOH/CH_2Cl_2 as the mobile phase to provide 0.03 g (66%) of a yellowish oily product. ^{1}H NMR (DMSO-*d*6) δ ppm 7.65 (d, *J* = 10.0 Hz, 1H), 7.60 (d, *J* = 10.0 Hz, 1H), 6.97 (d, *J* = 10.0 Hz, 1H), 6.92 (d, *J* = 5.0 Hz, 1H), 6.54 (m, 1H), 5.22 (d, *J* = 5.0 Hz, 1H), 4.50 (m, 2H), 4.32-4.25 (m, 2H), 3.47 (m, 1H), 3.33-3.30 (m, 3H), 3.22-3.15 (m, 4H), 2.86 (m, 6H), 2.65-2.52 (m, 3H), 2.42-2.40 (m, 2H), 2.33-2.24 (m, 5H), 2.07-2.04 (m, 3H), 1.86 (m, 3H), 1.70-1.56 (m, 10H), 1.46-1.42 (m, 48H), 1.37-1.20 (m, 8H), 0.92 (t, *J* = 5.0 Hz, 3H); ^{13}C NMR (DMSO-*d*6) δ ppm 173.6, 173.1, 172.6, 172.5, 172.4, 172.3, 171.9, 171.4, 157.1, 137.9, 137.6, 131.0, 130.0, 128.3, 92.5, 81.9, 81.8, 81.7, 81.6, 56.0, 55.7, 53.5, 53.1, 52.9, 50.6, 47.9, 47.3, 45.8, 39.1, 32.8, 32.5, 32.3, 31.6, 30.9, 28.8, 28.6, 28.2, 28.11, 28.0, 27.9, 26.8, 22.5, 22.4, 13.6. ESI-MS *m*/*z*: 702.4 $(M/2 + Na)^+$.

(14*S*, 18*S*)-9-(4-Iodobenzyl)-2,8,16-trioxo-1-(4,7,10-tris(carboxymethyl)-1,4,7,10-tetraazacyclododecan-1-yl)-3,9,15,17-tetraazaicosane-14,18,20-tricarboxylic acid (3)

A cold solution of 50% TFA/CH_2Cl_2 (2 ml) was added to **10** (0.06 g, 0.05 mmol) and the resultant solution stirred at RT for 2 h. The reaction mixture was concentrated, purified by C-18 flash column chromatography using 40-50% acetonitrile/water as the mobile phase, and the fractions lyophilized to provide 0.030 g (62%) of a white solid. ^{1}H NMR (DMSO-*d*6) δ ppm 12.65 (bs, 1H), 8.46 (s, 1H), 7.69 (d, *J* = 3.0 Hz, 2H), 7.01 (s, 2H), 6.33 (s, 2H), 4.47 (d, *J* = 4.0 Hz, 2H), 4.08 (s, 5H), 3.88 (s, 3H), 3.09 (m, 15H), 2.37 (s, 2H), 2.24 (s, 3H), 1.91 (s, 1H), 1.71-1.62 (m, 2H), 1.44 (m, 9H), 1.23 (s, 2H); ^{13}C NMR (DMSO-*d*6) δ ppm 174.5, 174.4, 174.1, 173.7, 171.9, 158.0, 157.3, 138.4, 137.4, 137.1, 129.9, 128.8, 118.2, 115.8, 92.9, 92.7, 54.7, 54.0, 52.7, 52.2, 52.1, 51.7, 50.6, 49.6, 48.2, 47.1, 46.7, 31.8, 31.4, 29.9, 28.4, 27.8, 27.5, 26.7, 22.5, 22.3, 22.2. HRESI-MS: calcd. For $C_{40}H_{62}IN_8O_{15}$ 1021.3374 $[M + H)^+$, found 1021.3373.

^{175}Lutetium (III) (14*S*, 18*S*)-9-(4-Iodobenzyl)-2,8,16-trioxo-1-(4,7,10-tris(carboxymethyl)-1,4,7,10-tetraazacyclododecan-1-yl)-3,9,15,17-tetraazaicosane-14,18,20-tricarboxylic acid (3-Lu)

A solution of **3** (7.92 mg, 0.008 µmol) in 25 µL DMSO was diluted with 0.2 M NH_4OAc, pH 4.5, (1 ml). To this, a solution of 2.7 mg (0.008 µmol) of $Lu(NO_3)_3.xH_2O$ in 540 µl of 0.1 M HCl was added and the mixture heated at 70-80°C for 1 h on a water bath. The product was purified by HPLC using a Phenomenex, Luna 10 x 250 mm, 10 µ column, gradient 20/80/0.1 to 90/10/0.1

MeCN/H_2O/TFA, 0-40min, flow 15ml/min, and concentrated to give 5.0 mg (42% yield). HRESI-MS: calcd. For $C_{40}H_{58}ILuN_8O_{15}$ 1193.2547 $[M+H]^+$, found 1193.2535.

Radiochemistry

(14*S*, 18*S*)-9-(4-^{125}I-Iodobenzyl)-2,8,16-trioxo-1-(4,7,10-tris(carboxymethyl)-1,4,7,10-tetraazacyclododecan-1-yl)-3,9,15,17-tetraazaicosane-14,18,20-tricarboxylic acid (^{125}I-3):

Compound 9 (200 µg, 0.13 mmol) of was dissolved in 100 µl methanol in a borosilicate screw cap vial. To this was added 2 µl glacial acetic acid and 266 MBq (7.2 mCi) of a solution of Na^{125}I (Perkin Elmer), followed by 25 µl of a solution consisting of 1 mg N-chlorosuccinimide in 1 ml methanol. The vial was capped, shaken, and allowed to stand at RT for 20 min. The reaction mixture was concentrated to almost dryness with a stream of nitrogen and gentle heating. Trifluoroacetic acid (200 µl) was added and the vial was heated at 70°C for 45 min. The mixture was concentrated with a stream of nitrogen, the residue redissolved in 2 ml 20% acetonitrile in water, and purified by radio-HPLC. For this, a Phenomenex Luna C18 column (250 × 10 mm, 10 micron) was eluted at a flow rate of 4 ml/min with a gradient consisting of 0.1% TFA in each water (solvent A) and acetonitrile (solvent B); the proportion of B was linearly increased from 15% to 50% over 30 min. Under these conditions, **^{125}I-3** eluted with a retention time of 17 min and 133 MBq (3.6 mCi) was collected. Pooled HPLC fractions containing **^{125}I-3** were diluted to 20 ml with water and loaded onto a Waters Oasis HLB Sep-Pak. The cartridge was washed with 5 ml water, dried with a stream of nitrogen, and the product was eluted with 2 ml ethanol. The eluent was concentrated with a stream of nitrogen and the residual activity either diluted with saline for biodistribution studies or carried over for the synthesis of **^{125}I-3-Lu**.

^{175}Lutetium (III) (14*S*, 18*S*)-9-(4-^{125}I-Iodobenzyl)-2,8,16-trioxo-1-(4,7,10-tris(carboxymethyl)-1,4,7,10-tetraazacyclododecan-1-yl)-3,9,15,17-tetraazaicosane-14,18,20-tricarboxylic acid (^{125}I-3-Lu):

Method A. To **^{125}I-3** prepared above was added 150 µl 0.1M NaOAc (pH 4.5), and 25 µl 5 mM $Lu(NO_3)_3$ in 0.1M HCl and the solution mixed by a micropipette. This solution was heated at 70°C for 20 min, quenched with 100 µl 5 mM EDTA, diluted with 600 µl water and purified by HPLC. For this, a Phenomenex Luna C18 column (250 × 10 mm, 10 micron) was eluted at a flow rate of 4 ml/min with a gradient consisting of 0.1% TFA in both water (solvent A) and acetonitrile (solvent B); the proportion of B was linearly increased from15% to 40% over 30 min. Under these conditions, **^{125}I-3-Lu** and **^{125}I-3** eluted at 21.5 min and 20.5 min, respectively. An activity amount of 104 MBq (2.8 mCi) of **^{125}I-3-Lu** was collected with a molar activity of 2000 Ci/mmol. Pooled HPLC fractions containing **^{125}I-3-Lu** were diluted to 20 ml with water, and loaded onto a Waters Oasis HLB Sep-Pak. The cartridge was, washed with 5 ml water, dried with a stream of nitrogen and the product eluted with 2 ml ethanol. The ethanolic eluate was concentrated using a stream of nitrogen and the residual activity diluted with saline for use in biological studies.

Method B. Compound **9** (280 µg, 184 nmol) was placed in a borosilicate screw-cap vial. A solution of N-chlorosuccinimide in methanol (0.2 mg in 200 µl) was added to the above followed by 407 MBq (11 mCi) of Na^{125}I (Perkin Elmer) and 8 µl of glacial acetic acid. The vial was capped, shaken and allowed to stand at room temperature for 10 min. The reaction mixture was concentrated to almost dryness using a stream of nitrogen at 57-60°C. A 95:5 mixture of trifluoroacetic acid:water

(200 µl) was added to the above and the vial was heated at 60°C for 30 min. The volatiles were evaporated with a stream of nitrogen at 57-60°C. A mixture of 350 µl 0.1M NaOAc (pH 4.5) and 65 µl of 5 mM $Lu(NO_3)_3$ (325 mmol) in 0.1M HCl was added to the above and the combined mixture was blended using a micropipette. The resultant solution was heated at 60°C for 20 min, quenched with the addition of 100 µl 5 mM EDTA, diluted with 600 µl water and purified by radio-HPLC. For this, a Phenomenex Luna C18 column (250 × 4.6 mm, 10 micron) was eluted at a flow rate of 1 ml/min with a gradient consisting of 0.1% TFA in both water (solvent A) and acetonitrile (solvent B); the proportion of B was linearly increased from 15% to 40% over 30 min. Under these conditions, 233 MBq (6.3mCi) of **^{125}I-3-Lu** eluted at 22.5 min. Pooled HPLC fractions containing **^{125}I-3-Lu** were diluted to 20 ml with water and loaded onto a Waters Oasis HLB light Sep-Pak. The cartridge was washed with 5 ml water, dried with a stream of nitrogen, and the product activity eluted with 0.5 ml ethanol. For use in biological studies, the ethanol from the eluate was evaporated with a stream of nitrogen and the residual activity reconstituted in saline.

(14*S*, 18*S*)-9-(4-^{211}At-Astatobenzyl)-2,8,16-trioxo-1-(4,7,10-tris(carboxymethyl)-1,4,7,10-tetraazacyclododecan-1-yl)-3,9,15,17-tetraazaicosane-14,18,20-tricarboxylic acid (^{211}At-3)

A solution of ^{211}At in 0.02% NCS in methanol (444 MBq; 12 mCi) was added to **9 (**680 µg, 450 nmol) in a borosilicate screw cap vial followed by 2 µl glacial acetic acid. The vial was capped, shaken, and allowed to stand at RT for 20 min. The reaction mixture was concentrated to almost dryness using a stream of nitrogen with gentle heating. Trifluoroacetic acid (200 µl) was added to the residual activity and the vial heated at 70°C for 45 min. The volatiles were evaporated using a stream of nitrogen, the residue redissolved in 2 ml 20% acetonitrile in water, and purified by HPLC. For this, a Phenomenex Luna C18 column (250 × 10 mm, 10 micron) was eluted at a flow rate of 4 ml/min with a gradient consisting 0.1% TFA in both water (solvent A) and acetonitrile (solvent B); the proportion of B was linearly increased from 15% to 40% over 30 min. Under these conditions, (56 MBq; 1.5mCi) of **^{211}At-3** eluted at 20 min. Pooled HPLC fractions containing **^{211}At-3** were diluted to 20 ml with water and loaded onto a Waters Oasis HLB Sep-Pak. The cartridge was washed with 5 ml water, dried with a stream of nitrogen and the product was eluted with 2 ml ethanol. The ethanol from the eluate was evaporated with a stream of nitrogen and the activity carried over for the preparation of **^{211}At-3-Lu.**

^{175}Lutetium (III) (14*S*, 18*S*)-9-(4-[^{211}At]Astatobenzyl)-2,8,16-trioxo-1-(4,7,10-tris(carboxymethyl)-1,4,7,10-tetraazacyclododecan-1-yl)-3,9,15,17-tetraazaicosane-14,18,20-tricarboxylic acid (^{211}At-3-Lu)

Method A. A mixture of 150 µl 0.1M NaOAc (pH 4.5) and 25 µl 5 mM $Lu(NO_3)_3$ (125 mmol) in 0.1M HCl was added to the dry **^{211}At-3** and the solution was mixed by micropipette. It was heated at 70°C for 20 min and the reaction quenched with the addition of 100 µl 5 mM EDTA. After diluting with 600 µl water, the mixture was subjected to HPLC. For this, a Phenomenex Luna C18 column: (250 × 10 mm, 10 micron) was eluted at a flow rate of 4 ml/min with a gradient consisting of 0.1% TFA in both water (solvent A) and acetonitrile (solvent B); the proportion of B was linearly increased from 15% to 40% over 30 min. Under these conditions, 22 MBq (0.6 mCi) of **^{211}At-3-Lu** eluted at 19 min. Pooled HPLC fractions containing **^{211}At-3-Lu** were diluted to 20 ml with water and loaded onto a Waters Oasis HLB Sep-Pak. The cartridge was washed with 5 ml water, dried with a stream of nitrogen and the product eluted with 2 ml ethanol. This eluate was concentrated using a stream of nitrogen and the activity reconstituted in saline.

Method B. A solution of ^{211}At in 0.02% NCS in methanol (600 µl; 638 MBq/17.3 mCi) was added to 310 µg (204 nmol) of **9** in a borosilicate screw cap vial followed by 12 µl of glacial acetic acid. The vial was capped, shaken and allowed to stand at RT for 10 min. The reaction mixture was concentrated to dryness using a stream of nitrogen at 60°C. A 95:5 mixture of trifluoroacetic acid:water (200 µl) was added and the vial was heated at 60°C for 30 min. Volatiles were evaporated using a stream of nitrogen at 60°C. Sodium acetate buffer (0.1 M), pH 4.5 (500 µl) and a solution of $Lu(NO_3)_3$ in 0.1 M HCl (65 µl; 325 nmol) were added to the residue and the solution mixed with a micropipette. This solution was heated at 60°C for 20 min, 100 µl 5 mM EDTA added, and diluted with 600 µl water. The final product was purified by HPLC. For this, a Phenomenex Luna C18 column (250 × 4.6mm, 10 micron) was eluted at a flow rate of 1 ml/min with a gradient consisting of 0.1% TFA in both water (solvent A) and acetonitrile (solvent B); the proportion of B was linearly increased from15% to 40% over 30 min. Under these conditions, **^{211}At-3-Lu** (54 MBq/1.47 mCi) eluted at 22.5 min. Pooled HPLC fractions containing **^{211}At-VK-3-Lu** were diluted to 20 ml with water and loaded onto a Waters Oasis HLB light Sep-Pak. The cartridge was washed with 5 ml water, dried with a stream of nitrogen, and the product eluted with 0.5 ml ethanol. This eluate was concentrated using a stream of nitrogen and the activity reconstituted in saline.

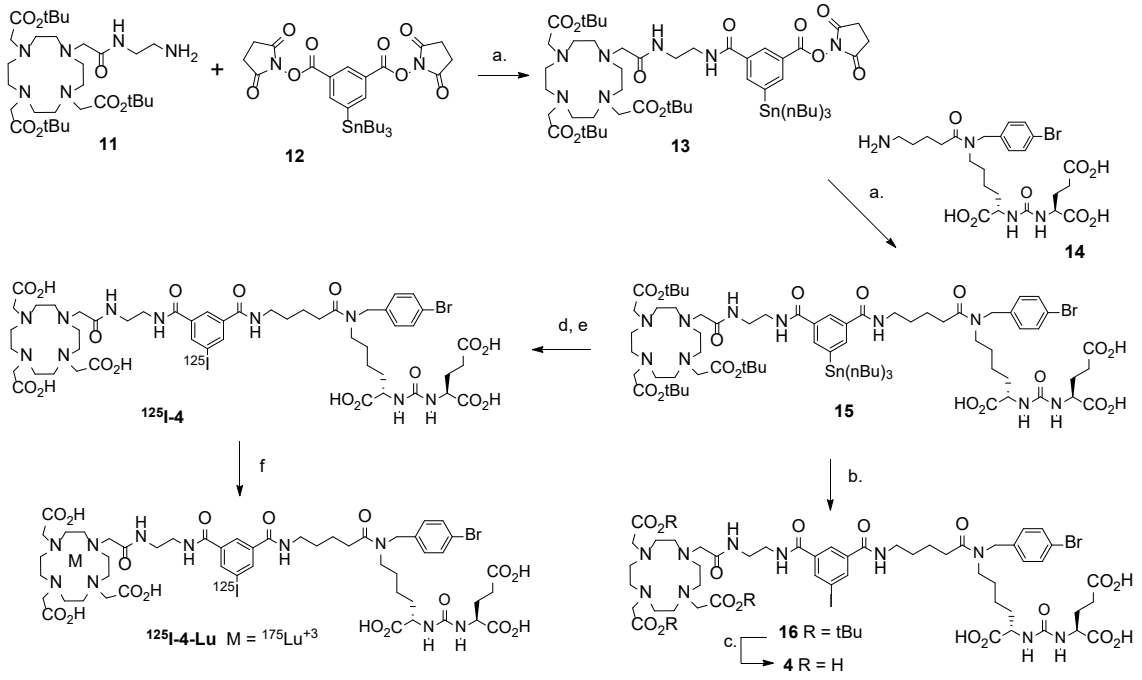

Synthesis of Radiolabeling precursor **15**, **4**, **^{125}I-4** and **^{125}I-4-Lu**. Reagents and conditions. a. triethylamine, DMSO, room temp. 2H; b. iodine, methylene chloride, room temp, 2H; c. 1/1 trifluoroacetic acid/methylene chloride,room temp. 2H; d. $Na^{125}I$, N-chlorosuccinimide, glacial acetic acid, methanol, room temperature 20 min; e. concentrated formic acid, 60°C, 1H; f. i. 0.1M sodium acetate, pH 4.5, 5mM $^{175}Lu(NO_3)_3$ in 0.1M HCl, 60°C, 20 min, ii. 5mM EDTA.

Tri-*tert*-butyl 2,2',2''-(10-(2-((2-(3-(((2,5-dioxopyrrolidin-1-yl)oxy)carbonyl)-5-(tributylstannyl)benzamido)ethyl)amino)-2-oxoethyl)-1,4,7,10-tetraazacyclododecane-1,4,7-triyl)triacetate (13).

A mixture of 2-aminoethyl-mono-amide-DOTA-tris(t-Bu ester) (**11**) (0.05 g, 0.07 mmol), bis(2,5-dioxopyrrolidin-1-yl) 5-(tri-n-butylstannyl)isophthalate (**12**) (0.05 g, 0.07 mmol) [3] and Et_3N (0.02

g, 0.22 mmol) in DMSO was stirred at RT for 2 h. The reaction mixture was concentrated and purified by flash column chromatography using 2% MeOH/CH_2Cl_2 as mobile phase to produce 0.03 g (38%) of oily material. ^{1}H NMR ($CDCl_3$) δ ppm 8.71 (s, 1H), 8.42 (s, 1H), 8.32 (s, 1H), 3.45 (s, 2H), 2.91 (bs, 4H), 2.61 (s, 47H, peak merged with DMSO), 1.63 (m, 1H), 1.54-1.44 (m, 7H), 1.33-1.23 (m, 12H), 1.11 (t, *J* = 5.0 Hz, 6H), 0.87 (t, *J* = 5.0 Hz, 9H). ESI-MS *m*/*z*: 1150.8 $(M + H)^+$.

(13*S*, 17*S*)-8-(4-Bromobenzyl)-1,7,15-trioxo-1-(3-(tributylstannyl)-5-((2-(2-(4,7,10-tris(2-(tert-butoxy)-2-oxoethyl)-1,4,7,10-tetraazacyclododecan-1-yl)acetamido)ethyl)carbamoyl)phenyl)-2,8,14,16-tetraazanonadecane-13,17,19-tricarboxylic acid (15)

A mixture of **13** (0.27 g, 0.23 mmol), **14** [4] (0.14 g, 0.23 mmol) and Et_3N (0.07 g, 0.70 mmol) was stirred in DMSO at RT for 2 h. The reaction mixture was concentrated, purified by C-18 column chromatography using 70-100% acetonitrile/water as mobile phase, and the chromatography fractions lyophilized to provide 0.1 g (25%) of a white solid. ^{1}H NMR ($CDCl_3$) δ ppm 8.69-8.55 (m, 3H), 8.31 (s, 1H), 8.00-7.94 (m, 2H), 7.60-7.56 (m, 1H), 7.50-7.48 (m, 1H), 7.41 (bs, 2H), 7.17-7.14 (m, 1H), 6.36-6.29 (m, 1H), 4.46 (s, 1H), 4.19 (bs, 2H), 4.10 (m, 2H), 3.11 (m, 6H), 2.94 (m, 5H), 2.41 (m, 1H), 2.27 (m, 2H), 1.93 (m, 1H), 1.61-1.55 (m, 10H), 1.49 (s, 16H), 1.41 (s, 28H), 1.33-1.28 (m, 11H), 1.14 (t, *J* = 5.0 Hz, 8H), 0.87 (t, *J* = 5.0 Hz, 9H). HRESI-MS: calcd. For $C_{74}H_{122}BrN_{10}O_{17}Sn$ 1621.7189 $[M+H]^+$, found 1621.7179.

(13*S*, 17*S*)-8-(4-Bromobenzyl)-1-(3-iodo-5-((2-(2-(4,7,10-tris(2-(tert-butoxy)-2-oxoethyl)-1,4,7,10-tetraazacyclododecan-1-yl)acetamido)ethyl)carbamoyl)phenyl)-1,7,15-trioxo-2,8,14,16-tetraazanonadecane-13,17,19-tricarboxylic acid (16)

Iodine (0.01 g, 0.09 mmol) was added to a solution of **15** (0.05 g, 0.03 mmol) in CH_2Cl_2 (2 ml) and the mixture stirred at RT for 2 h. The reaction mixture was concentrated and purified using a Waters C18 Sep-Pak Plus cartridge and 4060 acetonitrile/water as mobile phase to give 0.07g (yield > 100%) of a brown residue. This was used as such for next step. ESI-MS *m*/*z*: 1457.8 $(M + H)^+$.

(13*S*, 17*S*)-8-(4-Bromobenzyl)-1-(3-iodo-5-((2-(2-(4,7,10-tris(carboxymethyl)-1,4,7,10-tetraazacyclododecan-1-yl)acetamido)ethyl)carbamoyl)phenyl)-1,7,15-trioxo-2,8,14,16-tetraazanonadecane-13,17,19-tricarboxylic acid (4)

A chilled solution of 50% TFA/CH_2Cl_2 (2 ml) was added to crude **15** (0.07 g) and stirred at RT for 2 h. The reaction mixture was concentrated and purified using a Waters C18 Sep-Pak Plus cartridge and a step wise gradient of 40/60 to 20/80 water/acetonitrile to give 0.025g (62% yield) of **4** from **15**. ^{1}H NMR (CD_3CN + D_2O) δ ppm 8.24-8.22 (m, 1H), 8.13-8.11 (m, 1H), 7.89 (m, 1H), 7.53 (m, 1H), 7.46-7.40 (m, 2H), 7.08-7.05 (m, 2H), 4.48 (s, 1H), 4.43 (s, 1H), 4.16-4.13 (m, 2H), 3.64 (bs, 7H), 3.44 (s, 3H), 3.31 (m, 4H), 3.24-3.14 (m, 10H), 2.41 (m, 1H), 2.34-2.29 (m, 3H), 1.83-1.79 (m, 2H), 1.67-1.42 (m, 9H), 1.38-1.36 (m, 5H), 1.23 (m, 4H). HRESI-MS: calcd. For $C_{50}H_{71}BrIN_{10}O_{17}$ 1289.3221 $[M+H]^+$, found 1289.3243.

Radiochemistry

(13*S*, 17*S*)-8-(4-Bromobenzyl)-1-(3-^{125}I-iodo-5-((2-(2-(4,7,10-tris(carboxymethyl)-1,4,7,10-tetraazacyclododecan-1-yl)acetamido)ethyl)carbamoyl)phenyl)-1,7,15-trioxo-2,8,14,16-tetraazanonadecane-13,17,19-tricarboxylic acid (^{125}I-4)

Glacial acetic acid (2 µl) and 259 MBq (7 mCi) of ^{125}I were added to a solution of 200 µg (123 nmol) of **15** in 100 µl methanol in a borosilicate screw cap vial. This was followed by addition of N-chlorosuccinimide in methanol (25 µl; 1 mg/ml). The vial was capped, shaken, and allowed to stand at RT for 20 min. The reaction mixture was concentrated to almost dryness using a stream of nitrogen with gentle heating. Concentrated formic acid (200 µl) was added and the vial heated at 60°C for 60 min. After cooling, the contents were diluted to 1ml with water, and purified by HPLC. For this, a Phenomenex Luna C18 column (250 × 10 mm, 10 micron) was eluted at a flow rate of 4 ml/min with a gradient consisting of 0.1% TFA in both water (solvent A) and acetonitrile (solvent B); the proportion of B was linearly increased from 15% to 50% over 30 min. Under these conditions, **^{125}I-4** (37 MBq/1.0 mCi) eluted at a retention time of 21.5 min. Pooled HPLC fractions containing **^{125}I-4** were diluted to 20 ml with water and loaded onto a Waters Oasis HLB Sep-Pak. The cartridge was washed with 5 ml water, dried with a stream of nitrogen, and the product eluted with 2 ml ethanol. The eluate was concentrated using a stream of nitrogen.

^{175}Lutetium (III) (13*S*, 17*S*)-8-(4-Bromobenzyl)-1-(3-^{125}I-iodo-5-((2-(2-(4,7,10-tris(carboxymethyl)-1,4,7,10-tetraazacyclododecan-1-yl)acetamido)ethyl)carbamoyl)phenyl)-1,7,15-trioxo-2,8,14,16-tetraazanonadecane-13,17,19-tricarboxylic acid (^{125}I-4-Lu)

Sodium acetate buffer (0.1 M), pH 4.5 (150 µl) and a 25 µl of a solution of 5 mM $Lu(NO_3)_3$ in 0.1M HCl were added to **^{125}I-4** and the solution mixed by a micropipette. This solution was heated at 60°C for 20 min, 100 µl 5 mM EDTA added to quench the reaction, and the mixture diluted with 600 µl water and purified by HPLC. For this, a Phenomenex Luna C18 column (250 × 10 mm, 10 micron) was eluted at a flow rate of 4 ml/min with a gradient consisting of 0.1% TFA in both water (solvent A) and acetonitrile (solvent B); proportion of B was linearly increased from 15% to 50% over 30 min. Under these conditions, the retention time of **^{125}I-4-Lu** and **^{125}I-4** was 22.5 and 21.5 min, respectively. Ten MBq (270 µCi) of **^{125}I-4-Lu** was obtained. Molar activity of **^{125}I-4-Lu** was estimated to be 24 TBq 645 Ci/mmol based on the standard curve for **4.** Pooled HPLC fractions containing **^{125}I-4-Lu** were diluted to 20 ml with water and loaded onto a Waters Oasis HLB Sep-Pak. The cartridge washed with 5 ml water, dried with a stream of nitrogen and the product eluted with 2 ml ethanol. Ethanol from the eluent was evaporated using a stream of nitrogen.

Supplemental Figures

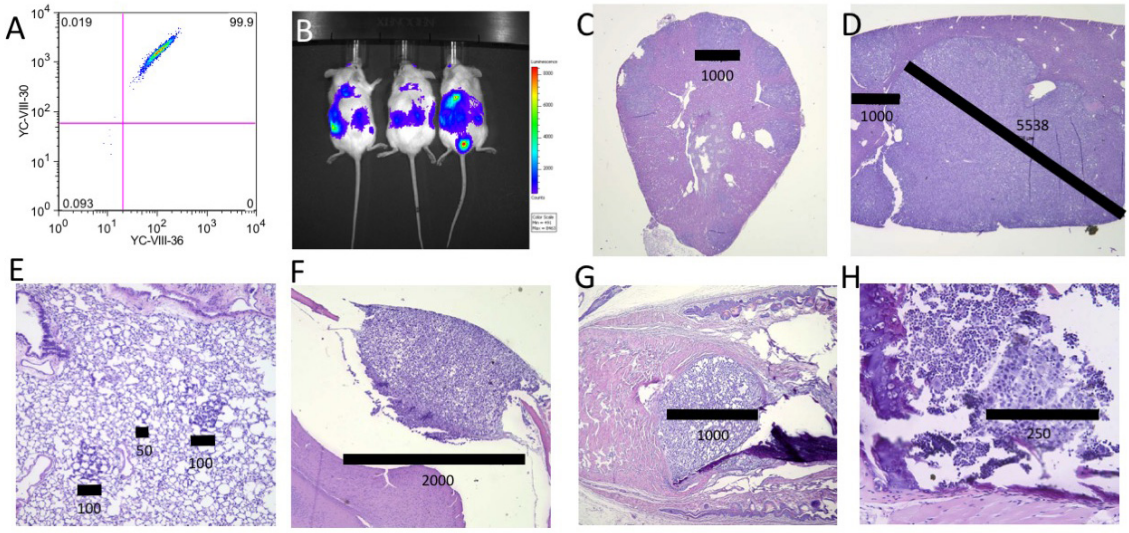

Supplemental Figure 1. PC3-ML-Luc cells were transduced with a lentiviral particle equipped to express the full-length PSMA and established a stable PSMA-expressing clone confirmed by fluorescence-activated cell sorting (FACS) (Supplemental Fig. 1A). Intravenous injection of PSMA-expressing PC3-ML-Luc cells (one million cells in 200 µL saline) to NSG (NOD-SCID IL2rγ^{null}) mice developed experimental metastatic lesions in kidney, liver, lung and bones. Tumor progression can be monitored non-invasively by in vivo bioluminescence imaging (BLI) (Supplemental Fig. 1B). The largest tumors (millimeters) and tumor burden are in the kidney (Supplemental Fig. 1C) and liver (Supplemental Fig. 1D). Lungs have abundant small (hundreds of micrometers) tumor metastases (Supplemental Fig. 1E). There were osteolytic bone lesions in skull (Supplemental Fig. 1F), baculum (Supplemental Fig. 1G), and sternum (Supplemental Fig. 1H).

Cell Uptake and Internalization

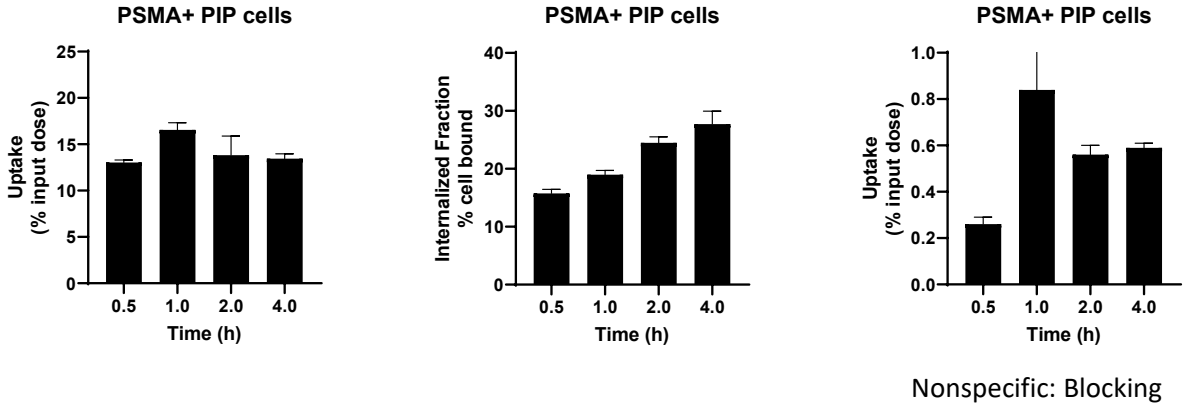

Supplemental Figure 2. Cell uptake and internalization results. See text and [5] for the experimental procedure.

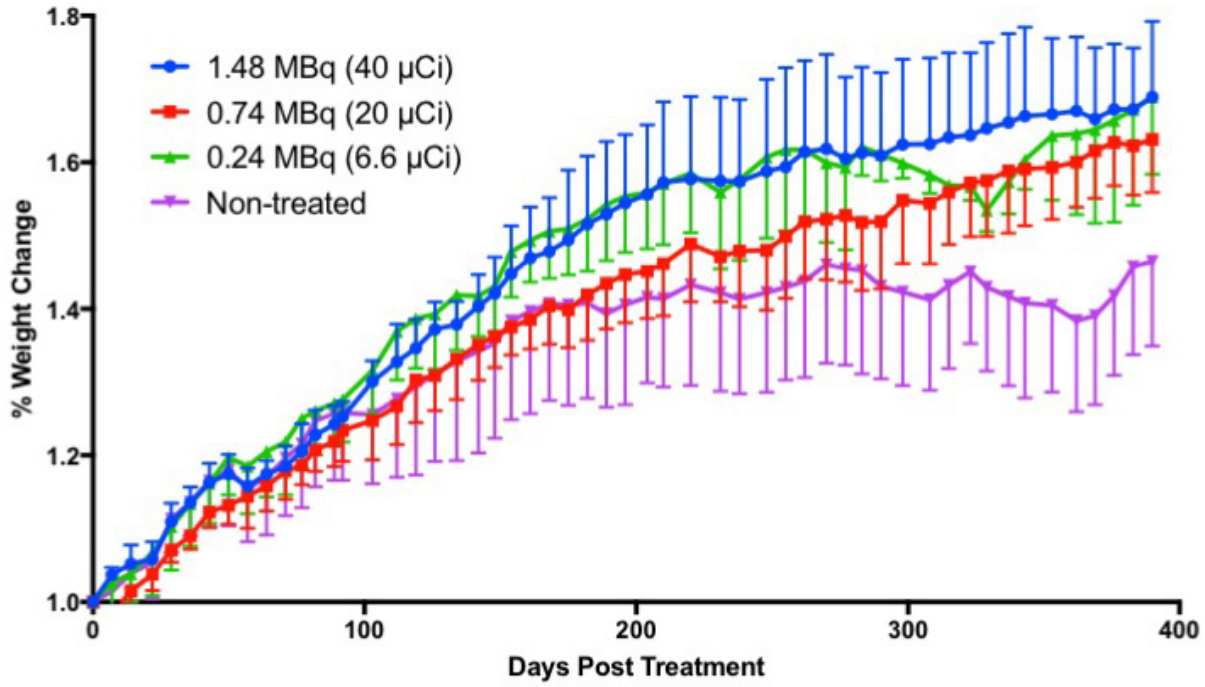

Supplemental Figure 3. Mice treated with varying doses of ^{211}At-3-Lu consistently gained weight. The body weight of each mouse was measured twice per week for 13 months. Only one data point per week is presented in the graph.

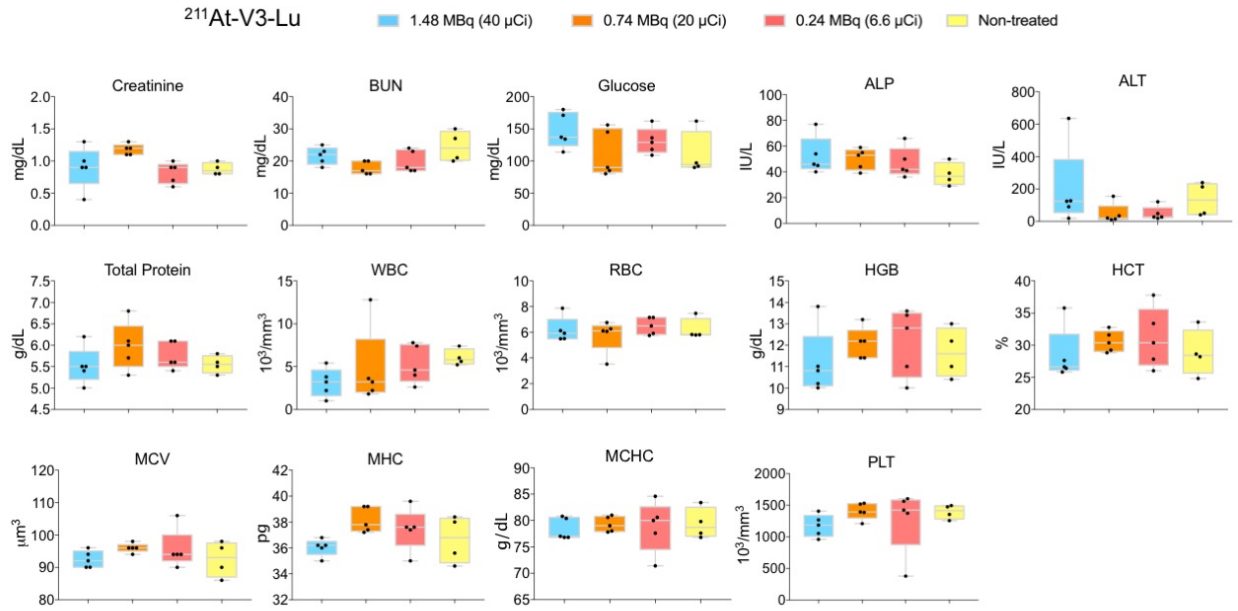

Supplemental Figure 4. Blood chemistry and complete blood count showed no treatment-related long-term toxicity. CD-1 mice treated with the indicated doses were maintained in a clean environment for 13 months. After euthanasia, whole blood was tested for indicated blood chemistry and CBC. Data are presented as box and whiskers plots. Each dot represents one animal. For the untreated group, one mouse was euthanized due to severe dermatitis, and data are from four remaining mice for the group. BUN: blood urea nitrogen, ALP: Alkaline Phosphatase, ALT: Alanine aminotransferase, WBC: white blood cells, RBC: red blood cells, HGB: hemoglobin, HCT: hematocrit, MCV: mean corpuscular volume, MCH: mean corpuscular hemoglobin, MCHC: mean corpuscular hemoglobin concentration, and PLT: platelet.

Biodistribution Tables

Supplemental Table 1. Biodistribution of ^{125}I-4 and ^{125}I-4-Lu (%ID/g)

	^{125}I-4			**^{125}I-4-Lu**		
Organ	**1 h**	**4 h**	**24 h**	**1 h**	**4 h**	**24 h**
blood	1.60 ± 0.26	0.49 ± 0.08	0.09 ± 0.02	2.44 ± 0.45	0.46 ± 0.16	0.06 ± 0.03
heart	1.60 ± 0.53	0.95 ± 0.26	0.17 ± 0.08	1.76 ± 0.38	0.57 ± 0.27	0.09 ± 0.04
lung	4.51 ± 0.63	2.35 ± 0.32	0.58 ± 0.20	4.83 ± 0.71	1.56 ± 0.48	0.15 ± 0.05
liver	0.90 ± 0.15	0.42 ± 0.21	0.09 ± 0.02	0.93 ± 0.13	0.24 ± 0.05	0.06 ± 0.02
spleen	70.0 ± 20.4	37.5 ± 8.9	4.90 ± 2.74	46.6 ± 17.3	15.7 ± 7.1	1.18 ± 0.41
pancreas	1.83 ± 0.28	1.46 ± 0.05	0.26 ± 0.07	1.36 ± 0.19	0.82 ± 0.73	0.04 ± 0.02
stomach	1.03 ± 0.12	0.96 ± 0.70	0.18 ± 0.07	0.93 ± 0.35	0.41 ± 0.18	0.07 ± 0.02
sm. Int.	0.76 ± 0.13	0.38 ± 0.08	0.08 ± 0.03	0.76 ± 0.21	0.21 ± 0.06	0.03 ± 0.02
lrg. Int.	1.20 ± 0.62	0.58 ± 0.19	0.12 ± 0.06	1.05 ± 0.20	0.26 ± 0.11	0.04 ± 0.01
fat	3.17 ± 0.73	4.14 ± 1.46	0.38 ± 0.28	3.45 ± 1.57	1.54 ± 0.92	0.62 ± 0.84
muscle	1.05 ± 0.21	0.64 ± 0.23	0.10 ± 0.05	1.00 ± 0.45	0.33 ± 0.18	0.03 ± 0.02
salivary gland	5.04 ± 0.87	3.48 ± 0.42	0.61 ± 0.16	4.10 ± 1.08	1.36 ± 0.46	0.15 ± 0.06
lacrimal gland	25.4 ± 4.1	15.8 ± 5.0	2.60 ± 0.76	18.7 ± 3.53	5.52 ± 2.52	0.70 ± 0.31
kidney	132 ± 19	166 ± 14	141 ± 18	145 ± 26	199 ± 34	50.4 ± 25.9
bladder	5.01 ± 2.86	2.41 ± 0.54	1.61 ± 0.75	3.05 ± 0.97	5.45 ± 6.01	2.78 ± 1.43
PC-3 PIP	44.7 ± 12.2	57.1 ± 15.9	54.1 ± 6.4	51.9 ± 15.0	60.1 ± 21.0	53.0 ± 8.0
PC-3 flu	2.05 ± 0.71	1.22 ± 0.28	0.20 ± 0.09	2.30 ± 0.90	0.75 ± 0.27	0.09 ± 0.02

Supplemental Table 2. Biodistribution of ^{125}I-3 and ^{125}I-3-Lu (%ID/g)

	^{125}I-3			**^{125}I-3-Lu**		
Organ	**1 h**	**4 h**	**24 h**	**1 h**	**4 h**	**24 h**
blood	1.08 ± 0.27	0.23 ± 0.03	0.02 ± 0.01	1.20 ± 0.39	0.06 ± 0.06	0.01 ± 0.00
heart	1.25 ± 0.46	0.24 ± 0.10	0.25 ± 0.02	0.71 ± 0.34	0.06 ± 0.02	0.01 ± 0.00
lung	3.45 ± 0.76	0.70 ± 0.19	0.07 ± 0.03	1.75 ± 0.54	0.16 ± 0.03	0.02 ± 0.00
liver	0.64 ± 0.17	0.16 ± 0.07	0.03 ± 0.01	0.48 ± 0.18	0.08 ± 0.07	0.02 ± 0.00
spleen	40.2 ± 16.4	4.69 ± 1.22	0.67 ± 0.39	7.41 ± 2.57	0.64 ± 0.20	0.13 ± 0.06
pancreas	1.53 ± 0.94	0.93 ± 1.45	0.03 ± 0.01	0.44 ± 0.11	0.16 ± 0.26	0.00 ± 0.00
stomach	1.12 ± 0.25	0.43 ± 0.19	0.05 ± 0.03	0.68 ± 0.38	0.10 ± 0.11	0.04 ± 0.01
sm. Int.	0.71 ± 0.29	0.17 ± 0.04	0.02 ± 0.02	0.45 ± 0.15	0.08 ± 0.09	0.01 ± 0.01
lrg. Int.	0.85 ± 0.38	0.19 ± 0.07	0.02 ± 0.01	0.64 ± 0.12	0.21 ± 0.33	0.02 ± 0.01
fat	3.18 ± 1.54	0.75 ± 0.30	0.49 ± 0.38	1.78 ± 1.12	0.44 ± 0.33	0.09 ± 0.10
muscle	0.86 ± 0.51	0.14 ± 0.08	0.02 ± 0.01	0.48 ± 0.34	0.07 ± 0.10	0.00 ± 0.00
salivary gland	5.13 ± 3.36	0.72 ± 0.16	0.27 ± 0.29	0.95 ± 0.28	0.10 ± 0.05	0.03 ± 0.01
lacrimal gland	17.3 ± 6.03	1.86 ± 0.45	0.47 ± 0.21	4.11 ± 1.31	0.34 ± 0.09	0.06 ± 0.03
kidney	194 ± 25	162 ± 36	30.6 ± 14.0	180 ± 36	18.2 ± 3.9	3.30 ± 1.15
bladder	3.24 ± 1.77	4.88 ± 3.94	1.91 ± 2.24	30.6 ± 21.5	5.27 ± 3.19	0.34 ± 0.12
PC-3 PIP	58.6 ± 13.7	38.0 ± 12.8	51.0 ± 7.1	51.1 ± 8.5	27.8 ± 17.3	24.0 ± 6.2
PC-3 flu	1.45 ± 0.58	0.27 ± 0.06	0.04 ± 0.27	0.87 ± 0.27	0.30 ± 0.46	0.03 ± 0.01

Supplemental Table 3. Biodistribution of ^{211}At-3-Lu (%ID/g)			
Organ	**1 h**	**4 h**	**24 h**
blood	0.75 ± 0.18	0.11 ± 0.03	a
heart	0.28 ± 0.06	0.11 ± 0.04	a
lung	1.04 ± 0.38	0.27 ± 0.11	a
liver	0.40 ± 0.13	0.09 ± 0.04	a
spleen	2.51 ± 0.94	a	a
pancreas	0.14 ± 0.12	0.10 ± 0.16	a
stomach	0.39 ± 0.12	0.34 ± 0.20	a
sm. int.	0.19 ± 0.26	0.11 ± 0.09	a
large. int.	0.07 ± 0.13	0.12 ± 0.20	a
fat	0.40 ± 0.50	0.12 ± 0.12	a
muscle	0.14 ± 0.09	0.01 ± 0.10	a
salivary gland.	0.47 ± 0.19	0.19 ± 0.09	a
Lacrimal gland	0.82 ± 0.91	0.29 ± 1.14	a
Kidney	89.5 ± 42.7	2.12 ± 0.63	0.02 ± 0.20
bladder	15.7 ± 11.3	11.7 ± 11.2	a
PC-3 PIP	30.6 ± 4.8	17.1 ± 5.2	9.46 ± 0.96
PC-3 flu	0.43 ± 0.15	0.12 ± 0.04	a

a. < 0.05 %ID/g of ^{211}At in tissue

Supplemental Table 4. Tumor/Organ ratios for ^{125}I-4 and ^{125}I-4-Lu						
	^{125}I-4			**^{125}I-4-Lu**		
	1 h	**4 h**	**24 h**	**1 h**	**4 h**	**24 h**
blood	27 ± 5	103 ± 65	632 ± 108	21 ± 6	134 ± 43	1089 ± 556
liver	49 ± 9	142 ± 67	608 ± 130	57 ± 19	259 ± 105	893 ± 273
spleen	0.7 ± 0.2	1.3 ± 0.6	14 ± 8	1.3 ± 0.7	4.4 ± 2.9	49 ± 17
stomach	44 ± 14	71 ± 36	337 ± 106	65 ± 31	175 ± 90	859 ± 263
Sm. Int.	59 ± 17	136 ± 56	694 ± 209	73 ± 30	314 ± 182	2315 ± 1743
Lrg. Int.	46 ± 27	102 ± 66	553 ± 240	51 ± 17	253 ± 120	1333 ± 320
Sal. gland	9 ± 3	13 ± 5	92 ± 20	13 ± 6	47 ± 21	397 ± 178
Lac. gland	1.7 ± 0.3	2.8 ± 1.2	22 ± 5	2.7 ± 0.5	11 ± 4	89 ± 39
kidney	0.3 ± 0.1	0.2 ± 0.1	0.3 ± 0.1	0.4 ± 0.2	0.3 ± 0.1	1.3 ± 0.7

Supplemental Table 5. Tumor/Organ ratios for ^{125}I-3 and ^{125}I-3-Lu						
	^{125}I-3			**^{125}I-3-Lu**		
	1 h	**4 h**	**24 h**	**1 h**	**4 h**	**24 h**
blood	54 ± 6	166 ± 92	4077 ± 2880	46 ± 19	824 ± 496	4119 ± 1446
liver	92 ± 11	250 ± 96	1663 ± 560	118 ± 49	575 ± 404	1276 ± 386
spleen	1.6 ± 0.4	6.8 ± 4.1	96 ± 55	5.8 ± 3.5	43 ± 25	213 ± 119
stomach	52 ± 8	93 ± 29	1192 ± 572	92 ± 45	535 ± 345	657 ± 179
Sm int	88 ± 18	222 ± 54	3706 ± 1792	125 ± 48	813 ± 494	2127 ± 1137
Lrg int	76 ± 26	250 ± 171	5197 ± 5785	84 ± 30	551± 475	1309 ± 547
Sal gland	13 ± 5	53 ± 15	328 ± 186	58 ± 22	365 ± 264	985 ± 369
Lac gland	3.5 ± 0.6	17 ± 4	126 ± 58	13 ± 6	92 ± 60	479 ± 286
kidney	0.3 ± 0.04	0.2 ± 0.1	1.9 ± 0.8	0.3 ± 0.06	1.7 ± 1.1	8.0 ± 4.8

Supplemental Table 6. Tumor/Organ Ratio for ^{211}At-3-Lu			
organ	**1 h[b]**	**4 h[c]**	**24 h[d,g]**
blood	54 ± 24	189 ± 118	a
liver	75 ± 19	168 ± 118	a
spleen	11 ± 3	97 ± 137	a
stomach	84 ± 25	73 ± 91	a
Sm int	113 ± 51	99 ± 61 e	a
Lrg int	211 ± 151	84 ± 105 f	a
Sal gland	75 ± 34	129 ± 99	a
Lac gland	44 ± 26	164 ± 220	a
kidney	0.5 ± 0.2	7.8 ± 6.0	130 ± 113

a. < 0.05 %ID/g ^{211}At in tissue.
b. n = 4, no PSMA+ PC3 PIP tumor in mouse #2
c. n = 4, no PSMA+ PC3 PIP tumor in mouse #4
d. n = 3, no PSMA+ PC3 PIP tumor in mouse #3 and #4
e. no ^{211}At in small intestine in one mouse
f. no ^{211}At in large intestine in 2 mice
g. one mouse had very low uptake in PSMA+ PC3 PIP tumor (0.44 %ID/g), data included

Supplemental Table 7. Monthly urine protein values (mg/dL).

Treatment	Mouse #	Month1	Month2	Month3	Month4	Month5	Month6	Month7
^{211}At-3-Lu 1.48 MBq	Mouse 1	trace	trace	30	30	30	100	30
	Mouse 2	trace	30	30	100	30	30	30
	Mouse 3	trace	30	30	30	30	100	30
	Mouse 4	trace	30	30	30	30	100	30
	Mouse 5	30	30	30	30	30	100	30
^{211}At-3-Lu 0.74 MBq	Mouse 1	30	100	30	30	100	300	30
	Mouse 2	30	30	30	30	30	100	100
	Mouse 3	30	30	30	100	30	100	30
	Mouse 4	30	30	30	30	30	100	30
	Mouse 5	trace	30	300	30	30	100	30
^{211}At-3-Lu 0.24 MBq	Mouse 1	30	30	30	100	30	100	30
	Mouse 2	30	30	30	30	30	100	100
	Mouse 3	30	30	100	30	30	100	30
	Mouse 4	trace	30	30	100	30	100	100
	Mouse 5	trace	30	100	30	30	30	30
Non-treated	Mouse 1	trace	30	30	30	30	100	30
	Mouse 2	trace	30	30	30	30	30	30
	Mouse 3	trace	30	30	30	30	30	30
	Mouse 4	30	30	30	30	100	30	30
	Mouse 5	trace	30	30	30	30	100	30

Treatment	Mouse #	Month8	Month9	Month10	Month11	Month12	Month13
^{211}At-3-Lu 1.48 MBq	Mouse 1	30	100	30	30	30	30
	Mouse 2	30	100	100	30	30	30
	Mouse 3	30	30	100	30	30	30
	Mouse 4	30	30	30	30	30	30
	Mouse 5	30	30	30	30	30	30
^{211}At-3-Lu 0.74 MBq	Mouse 1	100	100	100	300	100	100
	Mouse 2	100	30	100	100	100	100
	Mouse 3	30	30	100	100	100	100
	Mouse 4	100	30	100	30	100	100
	Mouse 5	100	100	100	100	100	100
^{211}At-3-Lu 0.24 MBq	Mouse 1	100	100	100	100	100	30
	Mouse 2	100	100	100	100	100	100
	Mouse 3	100	100	100	100	100	100
	Mouse 4	100	100	100	100	100	100
	Mouse 5	100	30	100	30	100	

Non-treated	Mouse 1	100	100	300	300	30	30
	Mouse 2	100	30	100	100	30	30
	Mouse 3	100	30	300	100	N/A	N/A
	Mouse 4	100	30	30	30	30	300
	Mouse 5	100	30	30	30	30	100

Supplemental Table 8. Monthly urine specific gravity values (g/mL).

Treatment	Mouse #	Month1	Month2	Month3	Month4	Month5	Month6	Month7
^{211}At-3-Lu 1.48 MBq	Mouse 1	1.03	1.025	1.025	1.025	1.025	1.03	1.025
	Mouse 2	1.025	1.025	1.03	1.025	1.025	1.03	1.025
	Mouse 3	1.025	1.025	1.02	1.025	1.025	1.025	1.025
	Mouse 4	1.025	1.015	1.02	1.025	1.025	1.025	1.025
	Mouse 5	1.03	1.005	1.02	1.025	1.025	1.025	1.02
^{211}At-3-Lu 0.74 MBq	Mouse 1	1.025	1.025	1.015	1.02	1.015	1.015	1.025
	Mouse 2	1.03	1.025	1.02	1.02	1.025	1.025	1.02
	Mouse 3	1.025	1.025	1.025	1.025	1.03	1.025	1.025
	Mouse 4	1.025	1.015	1.01	1.02	1.02	1.025	1.025
	Mouse 5	1.03	1.025	1.025	1.025	1.025	1.025	1.025
^{211}At-3-Lu 0.24 MBq	Mouse 1	1.03	1.015	1.025	1.025	1.025	1.025	1.025
	Mouse 2	1.03	1.025	1.025	1.02	1.02	1.025	1.025
	Mouse 3	1.03	1.025	1.025	1.025	1.025	1.025	1.02
	Mouse 4	1.03	1.025	1.025	1.025	1.025	1.025	1.025
	Mouse 5	1.03	1.015	1.025	1.025	1.025	1.025	1.025
Non-treated	Mouse 1	1.03	1.025	1.025	1.02	1.025	1.015	1.025
	Mouse 2	1.025	1.025	1.025	1.03	1.025	1.03	1.025
	Mouse 3	1.03	1.025	1.03	1.03	1.03	1.03	1.025
	Mouse 4	1.025	1.025	1.03	1.03	1.03	1.03	1.025
	Mouse 5	1.025	1.02	1.03	1.03	1.025	1.03	1.025

Treatment	Mouse #	Month8	Month9	Monyj10	Month11	Month12	Month13
^{211}At-3-Lu 1.48 MBq	Mouse 1	1.025	1.025	1.025	1.03	1.03	1.025
	Mouse 2	1.025	1.025	1.025	1.03	1.025	1.025
	Mouse 3	1.025	1.025	1.025	1.025	1.025	1.025
	Mouse 4	1.025	1.02	1.01	1.01	1.025	1.025
	Mouse 5	1.025	1.025	1.025	1.025	1.025	1.025
^{211}At-3-Lu 0.74 MBq	Mouse 1	1.025	1.02	1.025	1.025	1.025	1.025
	Mouse 2	1.025	1.025	1.025	1.025	1.025	1.025
	Mouse 3	1.025	1.025	1.025	1.025	1.025	1.025
	Mouse 4	1.025	1.025	1.025	1.025	1.025	1.025
	Mouse 5	1.025	1.01	1.025	1.025	1.025	1.025
^{211}At-3-Lu 0.24 MBq	Mouse 1	1.025	1.015	1.01	1.02	1.025	1.02
	Mouse 2	1.025	1.025	1.025	1.025	1.025	1.025
	Mouse 3	1.025	1.025	1.02	1.025	1.025	1.025
	Mouse 4	1.025	1.025	1.025	1.01	1.025	1.025
	Mouse 5	1.025	1.025	1.025	1.025	1.025	

Non-treated	Mouse 1	1.025	1.025	1.025	1.02	1	1.03
	Mouse 2	1.025	1.025	1.025	1.025	1.03	1.03
	Mouse 3	1.025	1.025	1.025	1.025	N/A	N/A
	Mouse 4	1.025	1.025	1.025	1.025	1.03	1.25
	Mouse 5	1.025	1.025	1.025	1.025	1.025	1.025